

# Pinakiolite, $Mg_2Mn^{3+}O_2[BO_3]$ ; Warwickite, $Mg(Mg_{0.5}Ti_{0.5})O[BO_3]$ ; Wightmanite, $Mg_5(O)(OH)_5[BO_3] \cdot nH_2O$ : Crystal Chemistry of Complex 3 Å Wallpaper Structures

PAUL BRIAN MOORE, AND TAKAHARU ARAKI

Department of the Geophysical Sciences, The University of Chicago  
Chicago, Illinois 60637

## Abstract

Pinakiolite,  $Mg^{2+}_{1.68}Mn^{2+}_{0.09}Mn^{3+}_{1.00}Al^{3+}_{0.06}Fe^{3+}_{0.02}Mn^{4+}_{0.06}O_2[BO_3]$ ,  $Z = 8$ ,  $a$  21.79(1) Å,  $b$  5.977(5) Å,  $c$  5.341(5) Å, space group  $C2/m$ , is an ordered derivative of the hulsite structure. Jahn-Teller distortions of each of the three non-equivalent  $Mn^{3+}-O_6$  octahedra result in four equatorial distances ranging from 1.92 to 1.96 Å and two apical distances ranging from 2.23 to 2.26 Å.

Warwickite,  $Mg^{2+}_{1.33}Al^{3+}_{0.21}Fe^{3+}_{0.12}Ti^{4+}_{0.34}O[BO_3]$ ,  $Z = 4$ ,  $a$  9.197(7) Å,  $b$  9.358(9) Å,  $c$  3.085(2) Å, space group  $Pnam$ , exhibits preferential occupancy of  $Ti^{4+}$  in the  $M(1)$  position. The proposed distributions are  $M(1) = 0.50 Mg^{2+} + 0.12 Al^{3+} + 0.04 Fe^{3+} + 0.34 Ti^{4+}$  and  $M(2) = 0.83 Mg^{2+} + 0.09 Al^{3+} + 0.08 Fe^{3+}$ .

Wightmanite,  $Mg^{2+}_5(O)(OH)_5[BO_3] \cdot \sim 2H_2O$ ,  $Z = 4$ ,  $a$  13.46(2) Å,  $b$  3.102(5) Å,  $c$  18.17(2) Å,  $\beta$  91.60(5)°, space group  $I2/m$ , is an octahedral framework structure with large open channels. Two symmetry-independent sets of "bundles" occur in the structure where six  $Mg^{2+}$  coordinate to one  $O^{2-}$ . This average  $^{vi}Mg-^{vi}O$  2.17 Å distance is 0.06 Å greater than that found in  $MgO$ . A model of local cation-cation repulsion dependent on structure topology is advanced to explain this increase in average distance.

It is proposed that the kinds of octahedral cations distributed over the sites are dictated by minimization of average local deviations from electrostatic neutrality and the locations of the shared edges both parallel and perpendicular to the fiber repeat.

## Introduction

Pinakiolite, warwickite, and wightmanite belong to a large family of structures herein named the "3 Å fiber axis wallpaper structures." They are defined by the following properties:

1. No non-identical atoms overlap down the 3 Å projection,
2. the anions, and the anions only, of the idealized structures reside on the vertices of the regular triangular net,
3. the connectivity of each atom in the real structure is the same as that of the ideal structure, and
4. a cation occurs at the triangular centers (triangular coordination) or at the mid-point of a rhombus of two edge-sharing triangles (octahedral coordination).

Property 1 reduces the problem to a two dimensional map. Property 2 defines the basis vectors for generating the cells of the idealized structures. Property 3 defines continuous distortions of the structures into a mapping on the regular net (3,6), the net of equilateral triangles, six of which meet at each ver-

tex. Property 4 provides the combinatorial aspect of the problem. Since occupied rhombuses and triangles can join only according to certain rules and since some triangles are empty, the problem involves generations of patterns over the triangular net.

A large number of compounds, belong to this family. Included are periclase,  $MgO$  (down [110]); diaspore,  $AlO(OH)$ ; brucite,  $Mg(OH)_2$ ; rutile,  $TiO_2$ ; malachite,  $Cu_2(OH)_2[CO_3]$ ; sussexite,  $Mn^{2+}_2(OH)[B_2O_4(OH)]$ ; ludwigite,  $Mg_2Fe^{3+}O_2[BO_3]$ ; gageite,  $Mn^{2+}_7(O)(OH)_{12}$  (in part); fluorborite,  $Mg_3(OH,F)_3[BO_3]$ ; and many other more complicated structures.

Crystallochemically, the structures consist of infinite columns of edge-sharing octahedra where the octahedral edge and the column direction are the fiber axis repeat distance. Laterally, these columns may link by edge-sharing to other octahedral columns to form walls, bundles, rings, sheets, etc. In addition, triangular groups such as  $[BO_3]^{3-}$ ,  $[CO_3]^{2-}$ , etc, may link, with their planes normal to the fiber repeat, to the octahedral columns. Everywhere, the repeat distance is the octahedral edge: they are called

TABLE 1. Pinakiolite. Chemical Analyses as Elemental Percentages

	PINAKIOLITE			WARWICKITE		
	1	2	3	4	5	6
Ca	0.3	0.8	—	0.2	—	—
Mg	21.1	17.7	20.7	23.7	21.5	23.8
Mn	32.7	36.5	32.0	<0.1	—	—
Al	0.7	—	0.7	4.1	1.5	4.1
Fe	0.6	1.5	0.6	5.0	10.4	5.0
Ti	0.1	—	—	12.2	14.9	12.2
B	—	5.0	5.4	—	6.6	8.0
O	—	37.8	39.8	—	44.6	47.1

1. Electron probe analysis. A. J. Irving, analyst.
2. Flink (1890), recomputed as elements. Includes Pb 0.7%.
3. For composition  $Mg_{1.68}^{2+}Mn_{0.09}^{2+}Mn_{1.00}^{3+}Al_{0.05}^{3+}Fe_{0.02}^{3+}Mn_{0.06}^{4+}O_2[BO_3]$ .
4. Electron probe analysis. A. J. Irving, analyst.
5. Bradley (1909), recomputed as elements. Includes Si 0.6%.
6. For composition  $Mg_{1.33}^{2+}Al_{0.21}^{3+}Fe_{0.12}^{3+}Ti_{0.34}^{4+}O[BO_3]$ .

the 3 Å fiber axis structures because, in systems with oxide and hydroxyl anions, this distance approximately obtains. Because of the two-dimensional properties of their structures, they are like wallpaper designs.

Pinakiolite is of interest because it contains  $Mn^{3+}$ -O octahedra which show Jahn-Teller distortion. It is also an ordered derivative structure of hulsite, a compound which does not exhibit this polyhedral distortion due to a more isotropic electronic distribution for its cations. Wightmanite, a very complex structure with large channels, contains octahedral bundles or blocks of the periclase structure. We want to know how these bundles distort as a result of cation-cation repulsions. Warwickite,  $Mg(Mg_{0.5}Ti_{0.5})[BO_3]$ , belongs to a structure type where some compositions have ferromagnetic properties and affords a study into the unusual  $Mg^{2+}$ - $Ti^{4+}$  solid solutions.

Pinakiolite, warwickite, and wightmanite each present special problems, and we have elected to outline this study with discussion on each individual followed by a general discussion and conclusions appropriate to furthering of our knowledge for the entire family. The general problems of the combinatorial relationships of the 3 Å structures shall be offered by P.B.M. elsewhere.

### Chemical Compositions

Warwickite was analyzed by Bradley (1909), but it is uncertain if his elimination of some cations as spinel impurities was warranted. Pinakiolite was analyzed by Flink (1890), but his interpretation of valence states of cations can hardly apply. In addition, we were not certain if our crystals corresponded

to the same assemblage of these earlier studies. Accordingly, both the pinakiolite and warwickite in this study were analyzed by electron microprobe. We thank Dr. A. J. Irving, who performed analyses on these compounds utilizing synthetic ilmenite (Ti), anorthite (Al), olivine (Mg and Fe), and rhodonite (Mn) as standards. Dr. Irving informed us that both the pinakiolite and warwickite crystals were homogeneous throughout.

Results of the analyses for pinakiolite and warwickite and their older wet chemical analyses are provided in Table 1. To assess the nature of the valence states, we assumed that warwickite possessed filled sites, as suggested by the structure analysis, and that the compound has a cell formula  $4Me_2O[BO_3]$ . For pinakiolite with completely filled sites, the cell formula would be  $8Me_3O_2[BO_3]$  but in this compound we found evidence for the existence of some partially occupied sites and elected the stoichiometry  $8M_{2.90}O_2[BO_3]$ . An assumption was made: that the Mn(1), Mn(2), and Mn(3) sites were fully occupied by  $Mn^{3+}$  and that the remaining Mn possessed valence states  $Mn^{2+}$  and  $Mn^{4+}$  to exactly balance charge in the crystal. The site refinement and interatomic distance calculations supported these assumptions. In addition, the evidence for Jahn-Teller distortion appears only for the Mn(1), Mn(2), and Mn(3) positions. In both compounds, we did not find evidence against completely occupied  $O^{2-}$  and  $B^{3+}$  positions, so assumed full occupancy for these ions.

Objections may be raised that we propose a pinakiolite formula with manganese in three states of oxidation in the same crystal. In the ensuing more detailed discussion based on bond distances and site population refinements, the existence of  $Mn^{3+}$  is definitely established and almost certainly  $Mn^{4+}$ . Three valence states— $Mn^{2+}$ ,  $Mn^{3+}$ , and  $Mn^{4+}$ —have been established by our preliminary studies on langbanite. Although we have no conclusive external evidence that  $Fe^{3+}$  is the correct valence state in warwickite, this state not only more favorably agrees with charge balance but also appears to be corroborated by the interatomic distances.

The structure cell data and the cell contents in Table 2a (pinakiolite) and Table 2b (warwickite) agree fairly well with the results of the earlier measured specific gravities of the minerals. The observed mean indices of refraction are in good agreement with the calculated value based on the Gladstone-Dale relationship and the specific refractive energies

TABLE 2a. Pinakiolite. Structure Cell Parameters

	1	2	3
a (Å)	21.79 (1)	21.80	10.684 (3)
b (Å)	5.977 (5)	5.98	3.099 (1)
c (Å)	5.341 (5)	5.36	5.438 (2)
β	95.83° (5)	95.75	94.14 (3)
space group	C2/m	-	P2/m, P2
specific gravity	3.88*	-	4.5 - 4.6
formula	Mg <sup>2+</sup> <sub>1.68</sub> Mn <sup>2+</sup> <sub>0.09</sub> Mn <sup>3+</sup> <sub>1.00</sub> Al <sup>3+</sup> <sub>0.05</sub> Fe <sup>3+</sup> <sub>0.02</sub> Mn <sup>4+</sup> <sub>0.06</sub> O <sub>2</sub> [BO <sub>3</sub> ]		(Fe <sup>2+</sup> , Mg <sup>2+</sup> , Fe <sup>3+</sup> , Sn <sup>4+</sup> ) <sub>3</sub> O <sub>2</sub> [BO <sub>3</sub> ]
density (gm cm <sup>-3</sup> )	3.79		
formula*	Ca <sup>2+</sup> <sub>0.04</sub> Mg <sup>2+</sup> <sub>1.58</sub> Fe <sup>3+</sup> <sub>0.06</sub> Mn <sup>2+</sup> <sub>1.44</sub> O <sub>2</sub> [BO <sub>3</sub> ]		
density (gm cm <sup>-3</sup> )†	4.09		
Z	8	8	2

<sup>1</sup>This study.

<sup>2</sup>Takéuchi et al. (1950), a 5.36 Å, b 5.98, c 12.73, β 120°34', transformed by 102/010/100.

<sup>3</sup>Hulsite. Clark (1965).

\*Flink (1890). His analysis has been computed to Σ oxygen = 5.00

†Based on Flink's composition and the cell data of this study.

in Larsen and Berman (1934): <n><sub>obs</sub> = 2.01 and <n><sub>calc</sub> = 1.97 for pinakiolite and <n><sub>obs</sub> = 1.82 and <n><sub>calc</sub> = 1.85 for warwickite. Such consistencies for these complex oxides further substantiate our proposed formulae.

**Pinakiolite**

*Experimental*

A single crystal of pinakiolite was selected from a sample collected at Långban, Sweden, by P.B.M. It shows the characteristic tabular aspect of the development from which its name was derived. Single crystal investigation by precession photography revealed a larger C-centered cell compared to the primitive cell reported by Takéuchi, Watanabe, and Ito (1950). We provide results of this study in Table 2a and compare the Takéuchi cell.

The crystal, measuring 0.15 × 0.11 × 0.22 mm (b-axis = prism direction), was prepared for the PAILED automated diffractometer utilizing graphite monochromator, MoK<sub>α</sub> radiation, b-axis rotation. Reflections up to 2θ = 65° of the k = 0- to 8-levels were gathered with a scan rate of 2.5°/minute, half-angle scan of 1.8°, and background counts for 20 seconds on each side of the peak. One-thousand two-hundred and ninety-five independent reflections were processed to obtain F(obs); with μ = 57.7 cm<sup>-1</sup>,

using a polyhedral absorption correction by the Gaussian integral method (Burnham, 1966).

Three-dimensional Patterson synthesis followed by a trial β-general synthesis (Ramachandran and Srinivasan, 1970) provided the positions of all atoms. At this stage, it was necessary to select scattering curves for cation site refinements since the electron density distributions indicated some sites involved mixed occupancies. Our curves for Mn<sup>3+</sup>, Mn<sup>2+</sup>, Mg<sup>2+</sup>, and O<sup>1-</sup> derive from the tables of Cromer and Mann (1968) and for B<sup>+</sup> from Onken and Fischer (1968). Anomalous dispersion effects for Mn and Mg were included in the refinement.

TABLE 2b. Warwickite. Structure Cell Parameters

	1	2
a (Å)	9.197 (7)	9.20
b (Å)	9.358 (9)	9.45
c (Å)	3.085 (2)	3.01
space group		Pnam
formula	Mn <sup>2+</sup> <sub>1.33</sub> Al <sup>3+</sup> <sub>0.21</sub> Fe <sup>3+</sup> <sub>0.12</sub> Ti <sup>4+</sup> <sub>0.34</sub> O[BO <sub>3</sub> ]	
specific gravity*		3.35 ± 0.01
density (gm cm <sup>-3</sup> )		3.402
Z		4

<sup>1</sup>This study.

<sup>2</sup>Takéuchi et al. (1950).

\*Bradley (1909).

TABLE 3. Dependence of  $R(hkl)$  on  $F(hkl)$  for Pinakiolite, Warwickite, and Wightmanite

PINAKIOLITE				WARWICKITE				WIGHTMANITE			
$F(hkl)$	Number	$R(hkl)$		$F(hkl)$	Number	$R(hkl)$		$F(hkl)$	Number	$R(hkl)$	
Above 0.0	1288	0.089		Above 0.0	652	0.071		Above 0.0	1880	0.131	
" 7.0	986	0.074		" 5.8	403	0.052		" 4.1	1650	0.118	
" 20.9	689	0.060		" 11.6	229	0.047		" 12.4	1162	0.087	
" 41.9	344	0.044		" 19.2	106	0.044		" 24.8	536	0.051	
" 69.8	151	0.040						" 41.3	221	0.043	

### Refinement

We included 1288 independent reflections throughout refinement. Seven were omitted from refinement because of asymmetrical backgrounds. It was necessary to vary the occupancies of all sites containing the  $Mg^{2+}$  cations since their electron densities on the  $\gamma'$ -synthesis did not indicate completely occupied or pure  $Mg^{2+}$  sites. The  $Mn^{3+}$  sites, on the other hand, appeared completely occupied and afforded no evidence for the presence of other substituents.

Occupancy refinements are very sensitive to the difference between the two scattering curves. For species with similar curves, such as Mg and Al, the occupancy refinement is of little value but, in pinakiolite and warwickite, we consider differences between Mn and Mg and between Ti and Mg, respec-

tively. The isotropic thermal vibration parameter,  $B_s$ , takes on a different meaning: it combines the displacement from the centroid position due to thermal motion and displacements associated with bonds to the different cations occupying the site. In effect,  $B_s$  is an averaged residency parameter.

Least-squares full-matrix site multiplicity and mixed-scattering-curve refinement for Mg(1) through Mg(4), and atomic coordinate parameter and isotropic thermal vibration parameter refinements for all atoms converged to the distributions in  $R(hkl)$  as listed in Table 3a, with the final atom parameters in Table 4a. Table 5a provides the structure factor data. As interpreted,  $Mn(1) = Mn(2) = Mn(3) = Mn^{3+}$ ;  $Mg(1) = 0.81 Mg^{2+} + 0.19 Hole$ ;  $Mg(2) = 0.77 Mg^{2+} + 0.23 Hole$ ;  $Mg(3) = 0.84 Mg^{2+} + 0.16$

TABLE 4a. Pinakiolite. Site Multiplicities, Scattering Curves, Atomic Coordinates and Isotropic Thermal Vibration Parameters\*

Atom	Site Multiplicity	Scattering Curves	x	y	z	$B(\text{\AA}^2)$
Mn(1)	2	1.00 $Mn^{3+}$	0.5000	0.5000	0.0000	0.73(4)
Mn(2)	2	1.00 $Mn^{3+}$	.5000	.5000	.500	.70(3)
Mn(3)	4	1.00 $Mn^{3+}$	.2503(1)	.0000	.4993(2)	.57(2)
Mg(1)	2	0.83(3) $Mg^{2+}$ + 0.19 Hole	.5000	.0000	.0000	1.95(17)
Mg(2)	2	0.77(3) $Mg^{2+}$ + 0.23 Hole <sub>4+</sub>	.5000	.0000	.5000	2.06(18)
Mg(3)	4	0.84(1) $Mg^{2+}$ + 0.16(2) $Mn^{3+}$	.2500	.2500	.0000	.60(6)
Mg(4)	8	0.99(1) $Mg^{2+}$ + 0.01(1) $Fe^{3+}$ ?	.3869(1)	.2497(3)	.7072(3)	.64(5)
B(1)	4		.1344(4)	.0000	.8055(15)	.57(10)
B(2)	4		.3692(4)	.0000	.1986(17)	.85(11)
O(1)	4		.3972(3)	.5000	-.0162(11)	.73(8)
O(2)	4		.3959(3)	.5000	.4344(11)	.65(8)
O(3)	4		.1980(3)	.0000	.8332(10)	.74(7)
O(4)	4		.4014(3)	.0000	-.0166(12)	1.02(9)
O(5)	4		.4002(3)	.0000	.4397(12)	.94(9)
O(6)	4		.3058(3)	.0000	.1713(11)	.89(8)
O(7)	8		.5138(2)	.2755(6)	.2556(7)	.92(6)
O(8)	8		.2937(2)	.2502(6)	.6775(7)	.76(6)

\* Estimated standard errors refer to the last digit.

TABLE 4b. Warwickite. Site Multiplicities, Scattering Curves, Atomic Coordinates and Isotropic Thermal Vibration Parameters\*

Atom	Multiplicity	Scattering Curves	x	y	z	B (Å <sup>2</sup> )
M(1)	4	0.62 (2) Mg <sup>2+</sup> + 0.38 (2) Ti <sup>4+</sup>	0.1149 (1)	0.5695 (1)	1/4	0.72 (3)
M(2)	4	0.96 (1) Mg <sup>2+</sup> + 0.04 (1) Ti <sup>4+</sup>	.1032 (1)	.1899 (1)	1/4	0.44 (3)
B	4		.1673 (4)	.8753 (4)	1/4	0.66 (4)
O (1)	4		.0206 (3)	.8653 (3)	1/4	1.07 (4)
O (2)	4		.2488 (3)	.7507 (3)	1/4	1.01 (4)
O (3)	4		.2353 (3)	.0074 (3)	1/4	0.84 (4)
O (4)	4		.0118 (3)	.3842 (3)	1/4	0.87 (4)

\* Estimated standard errors refer to the last digit.

Mn<sup>4+</sup>; and Mg(4) = 0.99 Mg<sup>2+</sup> + 0.01 Mn<sup>4+</sup>. Our selection of Mn<sup>4+</sup> as the substituent cation derives from the average polyhedral interatomic distances discussed further on. The existence of partial occupancy for Mg(1) and Mg(2) conforms with the polyhedral interatomic averages for these sites, the discussion of which is deferred to a later section.

Based on the probe analysis of the pinakiolite, the cell contents are Mg<sup>2+</sup><sub>13.94</sub>Mn<sup>2+</sup><sub>0.72</sub>Mn<sup>3+</sup><sub>8.00</sub>Al<sup>3+</sup><sub>0.40</sub>

Fe<sup>3+</sup><sub>0.16</sub>Mn<sup>4+</sup><sub>0.48</sub>B<sub>8.00</sub>O<sub>40.00</sub>. Our proposed site distributions in the refinement lead to Mg<sup>2+</sup><sub>14.44</sub>(Hole)<sup>0+</sup><sub>0.84</sub>Mn<sup>3+</sup><sub>8.00</sub>Mn<sup>4+</sup><sub>0.72</sub>B<sub>8.00</sub>O<sub>40.00</sub>. It is impossible to propose distributions for the minor cations with any certitude. In the case of Mn<sup>2+</sup>, we find little evidence for its concentration at any particular site and conclude that it probably occurs distributed over the positions containing predominant Mg<sup>2+</sup>. For the ensuing discussions, we shall consider the limiting

TABLE 4c. Wightmanite. Parameters for the Ellipsoids of Vibration\*

Atom	i	μ <sub>i</sub>	θ <sub>ia</sub>	θ <sub>ib</sub>	θ <sub>ic</sub>	B (Å <sup>2</sup> )	Atom	i	μ <sub>i</sub>	θ <sub>ia</sub>	θ <sub>ib</sub>	θ <sub>ic</sub>	B (Å <sup>2</sup> )
Mg(1)		non-positive	definite			0.52 (3)	O (3)	1	0.109	12	90	80	0.81 (5)
								2	0.091	102	90	10	
								3	0.103	90	180	90	
Mg(2)	1	0.101	147 <sup>o</sup>	90 <sup>o</sup>	55 <sup>o</sup>	0.75 (3)	O (4)	1	0.110	58	90	34	0.79 (5)
	2	0.094	90	0	90			2	0.091	148	90	56	
	3	0.096	123	90	145			3	0.098	90	180	90	
Mg(3)	1	0.104	170	90	79	0.70 (3)	O (5)	1	0.101	34	90	58	0.71 (5)
	2	0.089	90	0	90			2	0.084	123	90	32	
	3	0.089	100	90	169			3	0.098	90	180	90	
Mg(4)	1	0.102	3	90	89	0.75 (3)	OH(1)	1	0.129	90	0	90	1.11 (6)
	2	0.091	93	90	1			2	0.100	14	90	78	
	3	0.098	90	180	90			3	0.124	76	90	168	
Mg(5)	1	0.092	119	90	27	0.52 (3)	OH(2)	1	0.117	44	90	48	0.74 (5)
	2	0.073	29	90	63			2	0.078	134	90	42	
	3	0.076	90	180	90			3	0.092	90	180	90	
B	1	0.121	85	90	7	0.80 (7)	OH(3)	1	0.125	90	0	90	1.05 (6)
	2	0.071	90	0	90			2	0.099	155	90	63	
	3	0.104	5	90	97			3	0.121	115	90	153	
O (1)	1	0.131	90	0	90	1.13 (8)	OH(4)	1	0.126	150	90	58	0.95 (5)
	2	0.098	101	90	9			2	0.098	90	0	90	
	3	0.127	169	90	99			3	0.102	120	90	148	
O (2)	1	0.143	175	90	84	1.27 (9)	OH(5)	1	0.108	90	0	90	0.86 (6)
	2	0.096	85	90	6			2	0.098	83	90	8	
	3	0.137	90	180	90			3	0.107	7	90	98	

\* i = ith principal axis; μ<sub>i</sub> = rms amplitude; θ<sub>ia</sub>, θ<sub>ib</sub>, θ<sub>ic</sub> = angles between ith principal axis and the cell axes a, b and c.

TABLE 5a. Structure Factors for Pinakiolite

H	K	L	FO	FC	H	K	L	FO	FC	H	K	L	FO	FC	H	K	L	FO	FC	H	K	L	FO	FC	H	K	L	FO	FC					
4	0	0	170.4	142.3	4	0	0	38.1	39.3	7	1	0	38.0	63.1	5	1	-1	7.1	3.0	12	4	0	131.1	131.1	14	0	-1	111.0	127.7	5	3	1	6.1	7.2
8	0	0	330.9	284.7	8	0	0	76.2	78.6	14	1	0	76.0	136.2	11	1	-1	14.1	5.4	18	2	0	262.1	262.1	16	0	-1	222.0	247.4	7	3	1	3.1	3.6
12	0	0	500.4	427.1	12	0	0	114.3	118.9	21	1	0	114.0	205.1	17	1	-1	21.1	7.7	24	2	0	393.1	393.1	18	0	-1	333.0	364.7	11	3	1	4.1	4.8
16	0	0	670.9	564.8	16	0	0	152.4	159.2	28	1	0	152.0	281.2	23	1	-1	28.1	9.9	30	2	0	524.1	524.1	20	0	-1	444.0	485.4	13	3	1	5.1	6.0
20	0	0	841.4	702.5	20	0	0	190.5	200.3	35	1	0	190.0	351.3	29	1	-1	35.1	11.9	36	2	0	655.1	655.1	24	0	-1	565.0	616.4	15	3	1	6.1	7.2
24	0	0	1011.9	840.2	24	0	0	228.6	241.7	42	1	0	228.0	421.4	35	1	-1	42.1	13.9	42	2	0	766.1	766.1	28	0	-1	676.0	737.4	17	3	1	7.1	8.4
28	0	0	1182.4	977.9	28	0	0	266.7	283.1	49	1	0	266.0	491.5	41	1	-1	49.1	15.9	48	2	0	877.1	877.1	32	0	-1	787.0	848.4	19	3	1	8.1	9.6
32	0	0	1352.9	1115.6	32	0	0	304.8	324.9	56	1	0	304.0	561.6	47	1	-1	56.1	17.9	54	2	0	988.1	988.1	36	0	-1	898.0	959.4	21	3	1	9.1	10.8
36	0	0	1523.4	1253.3	36	0	0	342.9	365.1	63	1	0	342.0	631.7	53	1	-1	63.1	19.9	60	2	0	1099.1	1099.1	40	0	-1	1009.0	1070.4	23	3	1	10.1	12.0
40	0	0	1693.9	1391.0	40	0	0	381.0	405.3	70	1	0	381.0	701.8	60	1	-1	70.1	21.9	66	2	0	1210.1	1210.1	44	0	-1	1119.0	1180.4	25	3	1	11.1	13.2
44	0	0	1864.4	1528.7	44	0	0	419.1	445.5	77	1	0	419.0	771.9	67	1	-1	77.1	23.9	72	2	0	1321.1	1321.1	48	0	-1	1229.0	1290.4	27	3	1	12.1	14.4
48	0	0	2034.9	1666.4	48	0	0	457.2	484.9	84	1	0	457.0	842.0	74	1	-1	84.1	25.9	78	2	0	1432.1	1432.1	52	0	-1	1339.0	1400.4	29	3	1	13.1	15.6
52	0	0	2205.4	1804.1	52	0	0	495.3	523.7	91	1	0	495.0	912.1	81	1	-1	91.1	27.9	84	2	0	1543.1	1543.1	56	0	-1	1449.0	1510.4	31	3	1	14.1	16.8
56	0	0	2375.9	1941.8	56	0	0	533.4	562.1	98	1	0	533.0	982.2	88	1	-1	98.1	29.9	90	2	0	1654.1	1654.1	60	0	-1	1559.0	1620.4	33	3	1	15.1	18.0
60	0	0	2546.4	2079.5	60	0	0	571.5	601.5	105	1	0	571.0	1052.3	95	1	-1	105.1	31.9	96	2	0	1765.1	1765.1	64	0	-1	1675.0	1736.4	35	3	1	16.1	19.2
64	0	0	2716.9	2217.2	64	0	0	609.6	639.9	112	1	0	609.0	1122.4	102	1	-1	112.1	33.9	102	2	0	1876.1	1876.1	68	0	-1	1791.0	1852.4	37	3	1	17.1	20.4
68	0	0	2887.4	2354.9	68	0	0	647.7	678.3	119	1	0	647.0	1192.5	109	1	-1	119.1	35.9	108	2	0	1987.1	1987.1	72	0	-1	1910.0	1972.4	39	3	1	18.1	21.6
72	0	0	3057.9	2492.6	72	0	0	685.8	717.1	126	1	0	685.0	1262.6	116	1	-1	126.1	37.9	114	2	0	2098.1	2098.1	76	0	-1	2029.0	2092.4	41	3	1	19.1	22.8
76	0	0	3228.4	2630.3	76	0	0	723.9	754.5	133	1	0	723.0	1332.7	123	1	-1	133.1	39.9	120	2	0	2209.1	2209.1	80	0	-1	2148.0	2216.4	43	3	1	20.1	24.0
80	0	0	3398.9	2768.0	80	0	0	762.0	793.7	140	1	0	762.0	1402.8	130	1	-1	140.1	41.9	126	2	0	2320.1	2320.1	84	0	-1	2267.0	2336.4	45	3	1	21.1	25.2
84	0	0	3569.4	2905.7	84	0	0	800.1	831.9	147	1	0	800.0	1472.9	137	1	-1	147.1	43.9	132	2	0	2431.1	2431.1	88	0	-1	2386.0	2456.4	47	3	1	22.1	26.4
88	0	0	3739.9	3043.4	88	0	0	838.2	870.1	154	1	0	838.0	1543.0	144	1	-1	154.1	45.9	138	2	0	2542.1	2542.1	92	0	-1	2505.0	2572.4	49	3	1	23.1	27.6
92	0	0	3910.4	3181.1	92	0	0	876.3	906.3	161	1	0	876.0	1613.1	151	1	-1	161.1	47.9	144	2	0	2653.1	2653.1	96	0	-1	2624.0	2692.4	51	3	1	24.1	28.8
96	0	0	4080.9	3318.8	96	0	0	914.4	944.9	168	1	0	914.0	1683.2	158	1	-1	168.1	49.9	150	2	0	2764.1	2764.1	100	0	-1	2743.0	2812.4	53	3	1	25.1	30.0
100	0	0	4251.4	3456.5	100	0	0	952.5	983.1	175	1	0	952.0	1753.3	165	1	-1	175.1	51.9	156	2	0	2875.1	2875.1	104	0	-1	2862.0	2920.4	55	3	1	26.1	31.2
104	0	0	4421.9	3594.2	104	0	0	990.6	1021.7	182	1	0	990.0	1823.4	172	1	-1	182.1	53.9	162	2	0	2986.1	2986.1	108	0	-1	2981.0	3038.4	57	3	1	27.1	32.4
108	0	0	4592.4	3731.9	108	0	0	1028.7	1060.1	189	1	0	1028.0	1893.5	179	1	-1	189.1	55.9	168	2	0	3097.1	3097.1	112	0	-1	3100.0	3158.4	59	3	1	28.1	33.6
112	0	0	4762.9	3869.6	112	0	0	1066.8	1101.5	196	1	0	1066.0	1963.6	186	1	-1	196.1	57.9	174	2	0	3208.1	3208.1	116	0	-1	3219.0	3278.4	61	3	1	29.1	34.8
116	0	0	4933.4	4007.3	116	0	0	1104.9	1142.9	203	1	0	1104.0	2033.7	193	1	-1	203.1	59.9	180	2	0	3319.1	3319.1	120	0	-1	3338.0	3398.4	63	3	1	30.1	36.0
120	0	0	5103.9	4145.0	120	0	0	1143.0	1184.3	210	1	0	1143.0	2103.8	200	1	-1	210.1	61.9	186	2	0	3430.1	3430.1	124	0	-1	3457.0	3518.4	65	3	1	31.1	37.2
124	0	0	5274.4	4282.7	124	0	0	1181.1	1225.7	217	1	0	1181.0	2173.9	207	1	-1	217.1	63.9	192	2	0	3541.1	3541.1	128	0	-1	3576.0	3638.4	67	3	1	32.1	38.4
128	0	0	5444.9	4420.4	128	0	0	1219.2	1267.1	224	1	0	1219.0	2244.0	214	1	-1	224.1	65.9	198	2	0	3652.1	3652.1	132	0	-1	3695.0	3758.4	69	3	1	33.1	39.6
132	0	0	5615.4	4558.1	132	0	0	1257.3	1311.5	231	1	0	1257.0	2314.1	221	1	-1	231.1	67.9	204	2	0	3763.1	3763.1	136	0	-1	3814.0	3874.4	71	3	1	34.1	40.8
136	0	0	5785.9	4695.8	136	0	0	1295.4	1365.9	238	1	0	1295.0	2384.2	228	1	-1	238.1	69.9	210	2	0	3874.1	3874.1	140	0	-1	3933.0	3994.4	73	3	1	35.1	42.0
140	0	0	5956.4	4833.5	140	0	0	1333.5	1420.3	245	1	0	1333.0	2454.3	235	1	-1	245.1	71.9	216	2	0	3985.1	3985.1	144	0	-1	4052.0	4114.4	75	3	1	36.1	43.2
144	0	0	6126.9	4971.2	144	0	0	1371.6	1474.7	252	1	0	1371.0	2524.4	242	1	-1	252.1	73.9	222	2	0	4096.1	4096.1	148	0	-1	4171.0	4234.4	77	3	1	37.1	44.4
148	0	0	6297.4	5108.9	148	0	0	1409.7	1529.1	259	1	0	1409.0	2594.5	249	1	-1	259.1	75.9	228	2	0	4207.1	4207.1	152	0	-1	4290.0	4354.4	79	3	1	38.1	45.6
152	0	0	6467.9	5246.6	152	0	0	1447.8	1583.5	266	1	0	1447.0	2664.6	256	1	-1	266.1	77.9	234	2	0	4318.1	4318.1	156	0	-1	4409.0	4464.4	81	3	1	39.1	46.8
156	0	0	6638.4	5384.3	156	0	0	1485.9	1637.9	273	1	0	1485.0	2734.7	263	1	-1	273.1	79.9	240	2	0	4429.1	4429.1	160	0	-1	4528.0	4584.4	83	3	1	40.1	48.0
160	0	0	6808.9	5522.0	160	0	0	1524.0	1692.3	280	1	0	1524.0	2804.8	270	1	-1	280.1	81.9	246	2	0	4540.1	4540.1	164	0	-1	4647.0	4704.4	85	3	1	41.1	49.2
164	0	0	6979.4	5659.7	164	0	0	1562.1	1746.7	287	1	0	1562.0	2874.9	277	1	-1	287.1	83.9	252	2	0	4651.1	4651.1	168	0	-1	4766.0	4824.4	87	3	1	42.1	50.4
168	0	0	7149.9	5797.4	168	0	0	1600.2	1801.1	294	1	0	1600.0	2945.0	284	1	-1	294.1	85.9	258	2	0	4762.1	4762.1	172	0	-1	4885.0	4944.4	89	3	1	43.1	51.6
172	0	0	7320.4	5935.1	172	0	0	1638.3	1855.5	301	1	0																						

of brucite topology. The  $[BO_3]^{3-}$  triangles fuse by corner-sharing to the zig-zag chains and the sheets.

The hulsite cell of Clark (1965) in Table 2a is related to that of pinakiolite. We illustrate the relationships between hulsite, pinakiolite, and the Takéuchi cell for the latter mineral as symmetry diagrams (Fig. 2). Ordering of atoms in the hulsite structure to form pinakiolite first proceeds via a doubling of the 3 Å fiber repeat axis, *b*. By ordering different atomic species along the fiber direction in an alternating fashion, two-fold rotors in hulsite (Fig. 2b) become 2<sub>1</sub>-screws (Fig. 2a) and it is possible to obtain the Takéuchi cell. Our pinakiolite cell, however, involves a doubling of the *a*-axis as well. Since many moderate to strong reflections in Table 5a involve odd *H*, we conclude that the data of Takéuchi, Watanabe, and Ito (1950) represent a subset of the full pinakiolite data.

We note from Table 5a that for  $(H, K, L) = 2N + 1$ , the structure factors are nearly zero. Define

$(2m + 1) = H$ ,  $(2n + 1) = K$ , and  $(2p + 1) = L$ , where  $(m, n, p)$  are integers. The structure factor for  $C2/m$  can be written  $8 \cos 2 \pi[(2m + 1)x + (2p + 1)z] \cos 2 \pi(2n + 1)y$ . Noting that  $y \equiv 0, 1/2$ ; and  $y \approx 1/4$  for Mg(4), O(7), and O(8)), the sine-cosine product terms are very nearly zero and the structure factor can be reduced to  $8 \cos 2 \pi(2m + 1)x \cos 2 \pi(2n + 1)y \cos 2 \pi(2p + 1)z \neq 0$ . For  $y \approx 1/4$ , the Mg(3), Mg(4), O(7), and O(8) contributions are very nearly zero. With  $x \approx 1/4$ , the Mn(3) contribution is very nearly zero. Mn(1), Mn(2), Mg(1), and Mg(2) are related pairwise by  $(x, y, z; x, y, 1/2 + z)$  and exactly cancel. We are left with the pairs B(1), B(2); O(1), O(4); O(2), O(5); and O(3), O(6) which are very nearly related by  $(x, y, z; x, 1/2 + y, z)$  and very nearly cancel. The existence of perceptible intensities for  $(H, K, L) = 2N + 1$  is a consequence of slight deviations from these identities.

TABLE 5a, Continued.

H	K	L	FO	FC	H	K	L	FO	FC	H	K	L	FO	FC	H	K	L	FO	FC	H	K	L	FO	FC					
23	3	-2	13.2	18.0	18	6	1	10.3	9.2	18	6	-2	10.7	10.4	7	2	21.0	22.2	3	5	-4	39.1	34.8	11	7	3	2.8	3.7	
25	3	-2	8.0	16.2	18	6	5	9.0	9.2	18	6	5	-4	10.4	10.4	7	2	21.0	21.0	3	5	-4	32.1	30.9	11	7	3	2.8	3.7
27	3	-2	25.5	26.4	20	4	1	95.7	67.8	18	6	-2	15.0	14.6	11	5	-4	19.5	19.8	7	5	-4	75.5	70.6	15	7	3	11.3	12.0
29	3	-2	17.0	18.2	22	4	1	32.2	28.0	22	4	1	32.2	28.0	15	3	-2	13.0	13.7	7	5	-4	13.8	13.7	15	7	3	11.3	12.0
31	3	-3	3.5	2.8	24	4	1	4.5	1.7	22	4	-2	29.2	23.0	15	3	-2	23.2	26.8	11	5	-4	31.1	31.1	5	7	-1	83.8	87.9
33	3	-3	3.5	1.2	26	4	1	13.5	10.6	26	4	-2	22.8	18.1	17	3	-2	29.3	29.4	11	5	-4	22.8	25.0	10	3	-1	101.4	31.8
35	3	-3	3.5	2.8	28	4	1	24.8	28.6	28	4	-2	27.8	24.8	17	3	-2	15.9	18.0	17	3	-2	26.0	22.3	12	4	-1	101.4	100.1
37	3	-3	3.5	1.2	30	4	1	89.2	92.1	30	4	-2	23.1	20.1	17	3	-2	23.0	20.5	17	3	-2	23.0	20.5	12	4	-1	36.5	37.1
39	3	-3	3.5	2.8	32	4	1	14.8	13.4	32	4	-2	10.7	9.7	17	3	-2	10.7	9.7	17	3	-2	10.7	9.7	12	4	-1	101.4	100.1
41	3	-3	3.5	1.2	34	4	1	24.8	28.6	34	4	-2	24.8	28.6	17	3	-2	15.9	18.0	17	3	-2	26.0	22.3	12	4	-1	101.4	100.1
43	3	-3	3.5	2.8	36	4	1	89.2	92.1	36	4	-2	23.1	20.1	17	3	-2	23.0	20.5	17	3	-2	23.0	20.5	12	4	-1	36.5	37.1
45	3	-3	3.5	1.2	38	4	1	14.8	13.4	38	4	-2	10.7	9.7	17	3	-2	10.7	9.7	17	3	-2	10.7	9.7	12	4	-1	101.4	100.1
47	3	-3	3.5	2.8	40	4	1	24.8	28.6	40	4	-2	24.8	28.6	17	3	-2	15.9	18.0	17	3	-2	26.0	22.3	12	4	-1	101.4	100.1
49	3	-3	3.5	1.2	42	4	1	89.2	92.1	42	4	-2	23.1	20.1	17	3	-2	23.0	20.5	17	3	-2	23.0	20.5	12	4	-1	36.5	37.1
51	3	-3	3.5	2.8	44	4	1	14.8	13.4	44	4	-2	10.7	9.7	17	3	-2	10.7	9.7	17	3	-2	10.7	9.7	12	4	-1	101.4	100.1
53	3	-3	3.5	1.2	46	4	1	24.8	28.6	46	4	-2	24.8	28.6	17	3	-2	15.9	18.0	17	3	-2	26.0	22.3	12	4	-1	101.4	100.1
55	3	-3	3.5	2.8	48	4	1	89.2	92.1	48	4	-2	23.1	20.1	17	3	-2	23.0	20.5	17	3	-2	23.0	20.5	12	4	-1	36.5	37.1
57	3	-3	3.5	1.2	50	4	1	14.8	13.4	50	4	-2	10.7	9.7	17	3	-2	10.7	9.7	17	3	-2	10.7	9.7	12	4	-1	101.4	100.1
59	3	-3	3.5	2.8	52	4	1	24.8	28.6	52	4	-2	24.8	28.6	17	3	-2	15.9	18.0	17	3	-2	26.0	22.3	12	4	-1	101.4	100.1
61	3	-3	3.5	1.2	54	4	1	89.2	92.1	54	4	-2	23.1	20.1	17	3	-2	23.0	20.5	17	3	-2	23.0	20.5	12	4	-1	36.5	37.1
63	3	-3	3.5	2.8	56	4	1	14.8	13.4	56	4	-2	10.7	9.7	17	3	-2	10.7	9.7	17	3	-2	10.7	9.7	12	4	-1	101.4	100.1
65	3	-3	3.5	1.2	58	4	1	24.8	28.6	58	4	-2	24.8	28.6	17	3	-2	15.9	18.0	17	3	-2	26.0	22.3	12	4	-1	101.4	100.1
67	3	-3	3.5	2.8	60	4	1	89.2	92.1	60	4	-2	23.1	20.1	17	3	-2	23.0	20.5	17	3	-2	23.0	20.5	12	4	-1	36.5	37.1
69	3	-3	3.5	1.2	62	4	1	14.8	13.4	62	4	-2	10.7	9.7	17	3	-2	10.7	9.7	17	3	-2	10.7	9.7	12	4	-1	101.4	100.1
71	3	-3	3.5	2.8	64	4	1	24.8	28.6	64	4	-2	24.8	28.6	17	3	-2	15.9	18.0	17	3	-2	26.0	22.3	12	4	-1	101.4	100.1
73	3	-3	3.5	1.2	66	4	1	89.2	92.1	66	4	-2	23.1	20.1	17	3	-2	23.0	20.5	17	3	-2	23.0	20.5	12	4	-1	36.5	37.1
75	3	-3	3.5	2.8	68	4	1	14.8	13.4	68	4	-2	10.7	9.7	17	3	-2	10.7	9.7	17	3	-2	10.7	9.7	12	4	-1	101.4	100.1
77	3	-3	3.5	1.2	70	4	1	24.8	28.6	70	4	-2	24.8	28.6	17	3	-2	15.9	18.0	17	3	-2	26.0	22.3	12	4	-1	101.4	100.1
79	3	-3	3.5	2.8	72	4	1	89.2	92.1	72	4	-2	23.1	20.1	17	3	-2	23.0	20.5	17	3	-2	23.0	20.5	12	4	-1	36.5	37.1
81	3	-3	3.5	1.2	74	4	1	14.8	13.4	74	4	-2	10.7	9.7	17	3	-2	10.7	9.7	17	3	-2	10.7	9.7	12	4	-1	101.4	100.1
83	3	-3	3.5	2.8	76	4	1	24.8	28.6	76	4	-2	24.8	28.6	17	3	-2	15.9	18.0	17	3	-2	26.0	22.3	12	4	-1	101.4	100.1
85	3	-3	3.5	1.2	78	4	1	89.2	92.1	78	4	-2	23.1	20.1	17	3	-2	23.0	20.5	17	3	-2	23.0	20.5	12	4	-1	36.5	37.1
87	3	-3	3.5	2.8	80	4	1	14.8	13.4	80	4	-2	10.7	9.7	17	3	-2	10.7	9.7	17	3	-2	10.7	9.7	12	4	-1	101.4	100.1
89	3	-3	3.5	1.2	82	4	1	24.8	28.6	82	4	-2	24.8	28.6	17	3	-2	15.9	18.0	17	3	-2	26.0	22.3	12	4	-1	101.4	100.1
91	3	-3	3.5	2.8	84	4	1	89.2	92.1	84	4	-2	23.1	20.1	17	3	-2	23.0	20.5	17	3	-2	23.0	20.5	12	4	-1	36.5	37.1
93	3	-3	3.5	1.2	86	4	1	14.8	13.4	86	4	-2	10.7	9.7	17	3	-2	10.7	9.7	17	3	-2	10.7	9.7	12	4	-1	101.4	100.1
95	3	-3	3.5	2.8	88	4	1	24.8	28.6	88	4	-2	24.8	28.6	17	3	-2	15.9	18.0	17	3	-2	26.0	22.3	12	4	-1	101.4	100.1
97	3	-3	3.5	1.2	90	4	1	89.2	92.1	90	4	-2	23.1	20.1	17	3	-2	23.0	20.5	17	3	-2	23.0	20.5	12	4	-1	36.5	37.1
99	3	-3	3.5	2.8	92	4	1	14.8	13.4	92	4	-2	10.7	9.7	17	3	-2	10.7	9.7	17	3	-2	10.7	9.7	12	4	-1	101.4	100.1
101	3	-3	3.5	1.2	94	4	1	24.8	28.6	94	4	-2	24.8	28.6	17	3	-2	15.9	18.0	17	3	-2	26.0	22.3	12	4	-1	101.4	100.1
103	3	-3	3.5	2.8	96	4	1	89.2	92.1	96	4	-2	23.1	20.1	17	3	-2	23.0	20.5	17	3	-2	23.0	20.5	12	4	-1	36.5	37.1
105	3	-3	3.5	1.2	98	4	1	14.8	13.4	98	4	-2	10.7	9.7	17	3	-2	10.7	9.7	17	3	-2	10.7	9.7	12	4	-1	101.4	100.1
107	3	-3	3.5	2.8	100	4	1	24.8	28.6	100	4	-2	24.8	28.6	17	3	-2	15.9	18.0	17	3	-2	26.0	22.3	12	4	-1	101.4	100.1
109	3	-3	3.5	1.2	102	4	1	89.2	92.1	102	4	-2	23.1	20.1	17	3	-2	23.0	20.5	17	3	-2	23.0	20.5	12	4	-1	36.5	37.1
111	3	-3	3.5	2.8	104	4	1	14.8	13.4	104	4	-2	10.7	9.7	17	3	-2	10.7	9.7	17	3	-2	10.7	9.7	12	4	-1	101.4	100.1
113	3	-3	3.5	1.2	106	4	1	24.8	28.6	106	4	-2	24.8	28.6	17	3	-2	15.9	18.0	17	3	-2	26.0	22.3	12	4	-1	101.4	100.1
115	3	-3	3.5	2.8	108	4	1	89.2	92.1	108	4	-2	23.1	20.1	17	3	-2	23.0	20.5	17	3	-2	23.0	20.5	12	4	-1	36.5	37.1
117	3	-3	3.5	1.2	110	4	1	14.8	13.4	110	4	-2	10.7	9.7	17	3	-2	10.7	9.7	17	3	-2	10.7	9.7	12	4	-1	101.4	100.1
119	3	-3	3.5	2.8	112	4	1	24.8	28.6	112	4	-2	24.8	28.6	17	3	-2	15.9	18.0	17	3	-2	26.0	22.3	12	4	-1	101.4	100.1
121	3	-3	3.5	1.2	114	4	1	89.2	92.1	114	4	-2	23.1	20.1															

Table 5b. Structure Factors for Warwickite

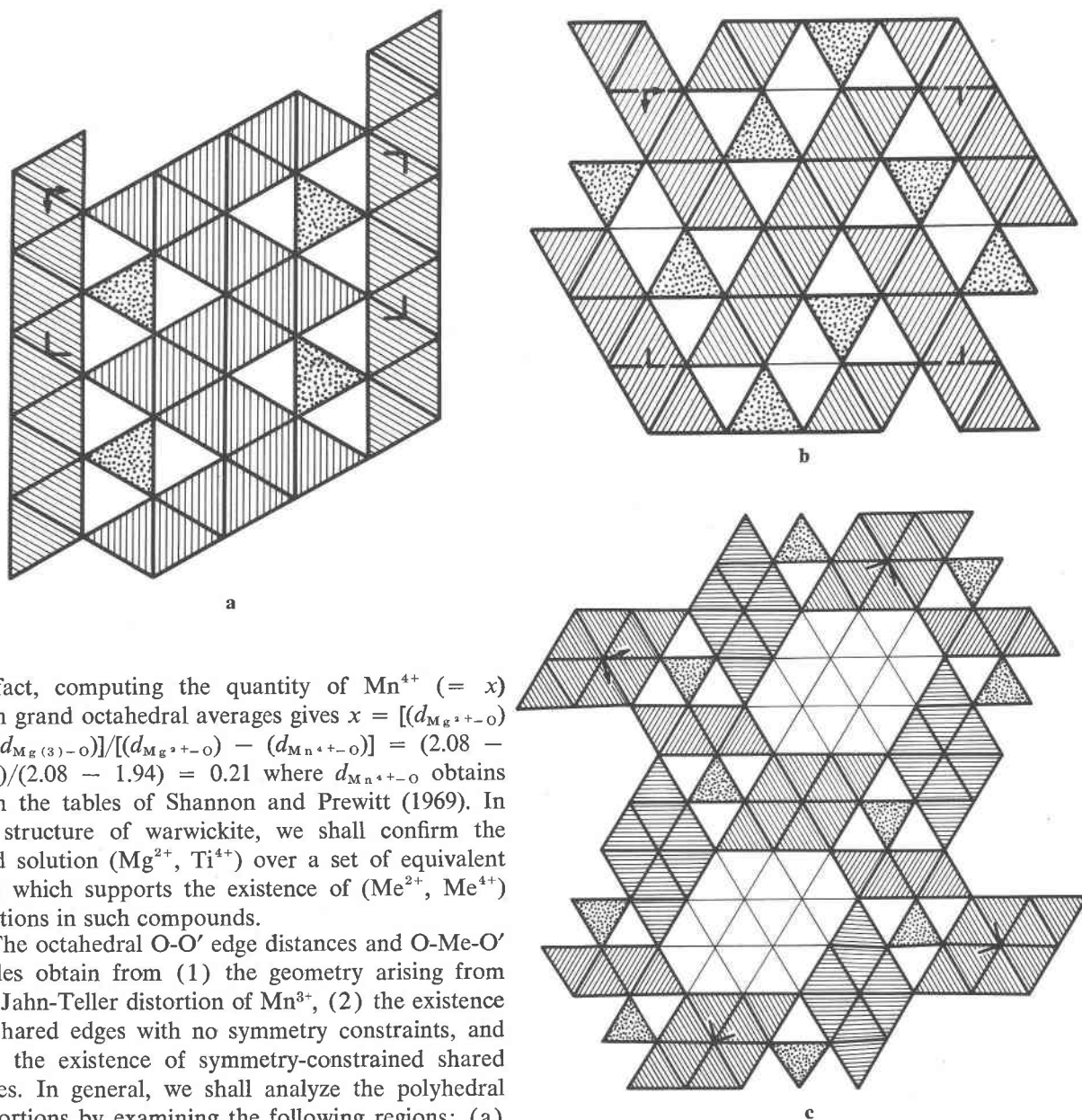
H	K	L	FD	FC	H	K	L	FD	FC	H	K	L	FD	FC	H	K	L	FD	FC	H	K	L	FD	FC
1	15	0	1.6	3.5	11	8	0	17.4	17.3	2	12	1	1.5	1.4	3	4	1	10.0	9.7	5	9	2	7.5	6.7
2	14	0	1.6	6.0	12	8	0	4.0	5.7	4	4	1	8.9	9.1	8	9	2	3.7	3.5	13	2	2	3.3	3.4
3	14	0	1.6	8.5	13	8	0	16.5	15.4	6	4	1	1.5	1.1	7	9	2	1.5	0.6	2	1	2	4.7	5.2
4	14	0	1.6	10.4	14	8	0	43.8	46.2	8	12	1	1.5	1.1	5	4	1	1.5	1.0	3	1	2	3.4	3.1
5	14	0	10.5	9.8	15	8	0	30.9	32.0	6	12	1	3.7	3.7	7	4	1	3.3	3.0	5	1	2	18.0	18.2
6	14	0	8.2	7.7	2	5	0	14.9	14.9	7	12	1	8.8	7.1	8	4	1	7.2	6.4	9	1	2	8.1	5.4
7	14	0	2.3	2.3	4	3	0	11.7	12.3	8	12	1	10.0	9.0	9	4	1	10.2	10.2	10	0	2	12.7	12.6
8	13	0	13.0	13.5	3	5	0	30.9	31.5	10	11	1	19.7	18.1	10	4	1	2.2	2.0	3	8	1	14.8	13.9
9	13	0	16.4	15.9	5	5	0	25.9	30.2	11	11	1	7.7	7.5	11	4	1	10.8	11.0	9	1	2	10.6	10.5
10	13	0	1.6	1.6	7	5	0	1.3	1.3	12	4	1	2.2	2.0	12	4	1	3.3	3.3	10	1	2	1.6	1.7
11	13	0	22.4	22.8	8	5	0	18.7	19.4	3	11	1	3.0	3.5	13	4	1	4.1	6.6	4	3	2	47.6	47.8
12	13	0	2.8	4.1	9	5	0	36.4	36.0	4	11	1	7.4	8.1	14	4	1	4.2	3.3	5	0	2	4.4	4.3
13	13	0	1.6	1.3	10	5	0	9.3	11.8	5	11	1	1.9	3.1	0	3	1	3.2	3.8	6	1	2	17.6	17.9
14	13	0	4.2	3.2	11	5	0	4.1	4.0	6	11	1	15.3	14.8	1	3	1	13.4	13.2	7	1	2	4.3	4.3
15	12	0	1.5	1.7	12	5	0	6.4	7.3	7	11	1	18.6	15.6	2	3	1	29.2	21.2	8	8	2	6.8	6.2
16	12	0	1.5	1.8	13	5	0	13.6	14.1	8	11	1	22.8	22.6	3	3	1	59.7	65.9	10	8	2	20.3	19.8
17	12	0	1.6	1.5	14	5	0	11.6	11.4	9	11	1	47.7	45.9	4	3	1	16.8	16.8	11	9	2	10.6	10.5
18	12	0	1.7	1.7	15	5	0	62.2	69.3	10	10	1	33.4	33.3	5	3	1	5.1	5.8	12	7	2	16.4	16.0
19	12	0	1.6	1.5	16	5	0	11.1	0.6	7	10	1	7.2	14.8	6	3	1	12.1	12.1	13	7	2	16.9	17.0
20	12	0	17.9	16.8	17	5	0	10.7	10.3	8	10	1	7.2	14.8	7	3	1	9.7	9.9	14	7	2	11.5	10.9
21	12	0	1.9	1.0	18	5	0	9.2	8.8	9	10	1	1.8	2.2	8	3	1	7.5	7.6	15	7	2	2.3	2.6
22	12	0	1.4	1.4	19	5	0	40.1	41.3	10	10	1	13.0	13.4	10	3	1	17.8	18.3	16	7	2	3.8	3.0
23	12	0	2.8	2.3	20	5	0	12.9	13.2	11	10	1	23.0	23.4	11	3	1	29.2	21.2	17	8	2	15.5	15.0
24	11	0	1.4	1.4	21	4	0	2.9	3.0	12	3	1	13.1	12.1	12	3	1	11.9	13.6	18	7	2	5.6	6.1
25	11	0	1.4	1.4	22	4	0	14.9	15.9	13	3	1	11.1	9.6	13	3	1	10.2	11.6	19	8	2	5.3	9.1
26	11	0	10.7	10.7	10	4	0	14.1	13.7	14	3	1	10.2	11.6	14	3	1	10.2	11.6	20	9	2	6.5	9.4
27	11	0	11.6	12.0	11	4	0	3.8	5.6	15	2	1	1.6	3.0	1	2	1	2.1	3.0	21	10	2	1.5	1.3
28	11	0	16.2	16.5	12	4	0	1.5	1.5	16	2	1	17.8	17.1	2	2	1	6.2	8.2	22	10	2	6.0	6.3
29	11	0	8.1	7.0	13	4	0	7.2	7.6	17	2	1	1.4	1.5	3	2	1	47.7	51.3	23	11	2	6.0	4.3
30	11	0	11.3	10.2	14	4	0	7.2	7.6	18	2	1	11.4	11.1	4	2	1	11.4	11.1	24	10	2	9.4	8.6
31	11	0	14.9	15.3	15	4	0	40.6	43.2	19	2	1	6.1	5.8	5	2	1	60.8	63.6	25	10	2	26.2	26.0
32	11	0	15.9	16.5	16	4	0	36.7	37.2	20	2	1	4.8	5.4	7	2	1	12.0	12.6	26	9	2	26.0	25.9
33	11	0	21.2	21.4	17	4	0	15.4	15.5	21	2	1	6.5	7.0	8	2	1	1.1	1.0	27	9	2	1.4	1.4
34	11	0	15.9	16.5	18	4	0	12.7	13.3	22	2	1	10.8	10.3	9	2	1	22.8	24.0	28	8	2	2.8	2.8
35	11	0	29.5	29.4	19	4	0	13.7	13.6	23	2	1	1.2	1.2	10	2	1	11.0	11.6	29	8	2	1.8	1.0
36	11	0	4.6	4.6	20	4	0	35.2	36.6	24	2	1	3.8	3.9	11	2	1	10.2	10.6	30	9	2	9.9	9.3
37	11	0	10.1	9.8	21	4	0	6.4	6.6	25	2	1	1.5	0.7	12	2	1	7.5	6.1	31	8	2	4.4	4.7
38	11	0	16.0	16.3	22	4	0	13.0	13.0	26	2	1	1.8	0.7	13	2	1	19.5	15.5	32	7	2	1.3	1.1
39	11	0	5.8	10.7	10	3	0	10.5	10.3	27	2	1	1.4	0.7	14	2	1	14.9	16.7	33	6	2	4.4	4.7
40	11	0	1.6	1.6	11	3	0	11.2	11.8	28	2	1	3.2	3.2	15	2	1	28.5	26.7	34	6	2	11.4	11.7
41	11	0	3.6	3.7	12	3	0	13.0	13.6	29	2	1	3.8	4.2	16	2	1	34.5	36.7	35	6	2	12.6	12.9
42	11	0	15.3	17.0	13	3	0	12.8	13.1	30	2	1	10.0	10.0	17	2	1	21.1	22.1	36	5	2	21.1	22.1
43	11	0	9.0	9.0	14	3	0	13.7	14.0	31	2	1	3.1	3.1	18	2	1	6.1	5.4	37	5	2	5.5	5.5
44	11	0	3.0	3.2	15	3	0	3.2	3.1	32	2	1	3.0	3.1	19	2	1	21.2	20.9	38	4	2	6.9	6.9
45	11	0	15.1	15.2	16	3	0	28.0	26.5	33	2	1	25.3	25.5	20	2	1	11.1	12.5	39	5	2	24.6	24.3
46	11	0	8.4	8.4	17	3	0	3.4	3.2	34	2	1	3.4	4.0	21	2	1	3.2	1.5	40	5	2	22.9	22.6
47	11	0	17.8	17.8	18	3	0	5.8	5.9	35	2	1	1.1	0.7	22	2	1	19.5	15.5	41	4	2	1.3	1.1
48	11	0	9.1	8.4	19	3	0	22.6	22.0	36	2	1	1.6	0.7	23	2	1	13.3	16.3	42	5	2	15.7	15.4
49	11	0	3.5	4.3	20	3	0	5.8	5.9	37	2	1	1.1	0.7	24	2	1	1.5	0.3	43	5	2	28.5	29.1
50	11	0	1.2	0.8	21	3	0	22.6	22.0	38	2	1	28.1	26.0	25	2	1	6.9	6.5	44	5	2	7.5	8.2
51	11	0	2.1	1.1	22	3	0	9.5	8.6	39	2	1	25.8	25.3	26	2	1	2.1	2.2	45	5	2	3.0	3.2
52	11	0	4.4	4.5	23	3	0	52.3	56.6	40	2	1	15.1	15.0	27	2	1	72.0	100.9	46	5	2	7.5	8.2
53	11	0	4.2	5.9	24	3	0	12.6	12.6	41	2	1	9.4	9.4	28	2	1	9.4	9.3	47	5	2	9.3	9.3
54	11	0	6.8	7.5	25	3	0	1.7	1.7	42	2	1	26.2	26.8	29	2	1	4.6	2.2	48	5	2	7.1	6.7
55	11	0	4.6	4.1	26	3	0	14.8	14.8	43	2	1	19.2	20.1	30	2	1	36.1	36.2	49	5	2	6.4	6.2
56	11	0	12.8	13.4	27	3	0	8.1	9.6	44	2	1	2.5	3.2	31	2	1	1.5	0.6	50	5	2	4.7	4.3
57	11	0	12.8	13.3	28	3	0	19.9	19.9	45	2	1	19.9	19.9	32	2	1	7.6	7.3	51	5	2	26.5	25.0
58	11	0	8.0	8.0	29	3	0	7.1	7.1	46	2	1	12.3	9.1	33	2	1	4.4	4.4	52	5	2	7.6	7.6
59	11	0	3.7	3.7	30	3	0	7.1	6.2	47	2	1	6.2	4.2	34	2	1	8.4	2.8	53	5	2	28.4	28.8
60	11	0	20.8	22.3	31	3	0	12.5	12.1	48	2	1	12.5	12.1	35	2	1	11.1	11.7	54	5	2	2.1	2.9
61	11	0	5.7	5.7	32	3	0	1.5	0.6	49	2	1	12.5	12.1	36	2	1	12.5	12.1	55	5	2	2.1	2.9
62	11	0	4.5	7.3	33	3	0	25.2	26.8	50	2	1	12.5	12.1	37	2	1	12.5	12.1	56	5	2	9.8	10.6
63	11	0	1.5	0.3	34	3	0	8.9	7.8	51	2	1	14.4	13.5	38	2	1	14.4	13.5	57	5	2	10.8	10.9
64	11	0	6.0	6.0	35	3	0	17.9	18.0	52	2	1	5.0	2.5	39	2	1	2.0	1.5	58	5	2	10.8	10.9
65	11	0	5.1	6.6	36	3	0	19.2	18.1	53	2	1	6.7	8.4	40	2	1	3.6	2.5	59	5	2	1.5	1.5
66	11	0	17.2	17																				

TABLE 5c. Structure Factors for Wightmanite

Table with columns H, K, L, FO, FC and rows of numerical data representing structure factors for Wightmanite. The table is organized into two main sections, each with its own set of column headers.

TABLE 5c, Continued.

H	K	L	FO	FC	H	K	L	FO	FC	H	K	L	FO	FC	H	K	L	FO	FC	H	K	L	FO	FC	H	K	L	FO	FC	H	K	L	FO	FC
14	2	2	30.5	-28.2	-7	2	9	28.0	-29.7	0	3	25	9.2	-1.5	10	3	13	12.9	14.2	-5	3	22	4.0	1.3	2	4	0	10.8	12.3	-8	4	9	13.1	-3.7
14	2	6	3.9	12.9	-7	2	13	16.1	19.9	1	3	6	94.1	58.0	10	3	17	31.7	22.3	-5	3	24	4.8	-1.6	2	4	5	5.8	6.2	0	5	3	5.0	-1.0
14	2	6	35.6	36.9	-7	2	15	4.2	5.4	1	3	6	94.1	58.0	10	3	17	31.7	22.3	-5	3	24	4.8	-1.6	2	4	5	5.8	6.2	0	5	3	5.0	-1.0
14	2	10	7.6	10.1	-7	2	17	1.0	7.9	1	3	10	51.2	-5.3	10	3	19	3.0	2.2	-6	3	3	4.4	-2.4	2	4	6	15.6	-16.6	0	5	3	20.2	18.6
14	2	12	3.6	3.3	-7	2	19	14.9	-11.8	1	3	12	7.0	-0.2	11	3	2	3.9	-5.1	-6	3	9	43.3	45.7	2	4	8	9.8	2.4	0	5	7	11.7	9.4
14	2	16	2.3	20.8	-7	2	21	15.5	-9.5	1	3	14	18.9	-22.0	11	3	2	3.9	-5.1	-6	3	9	48.4	49.7	2	4	12	19.6	22.0	0	5	9	16.6	14.3
14	2	18	3.3	10.8	-7	2	23	16.6	-18.7	1	3	16	7.6	-0.8	11	3	2	3.9	-5.1	-6	3	11	13.6	-10.7	3	4	1	1.3	-0.1	0	5	13	12.7	4.3
14	2	20	10.1	2.2	-8	2	25	17.0	-14.3	1	3	18	13.6	-0.8	11	3	2	3.9	-5.1	-6	3	13	11.2	-12.6	3	4	3	7.5	6.2	1	5	4	21.8	22.1
15	2	1	29.2	-28.7	-8	2	4	4.8	-1.5	2	3	22	12.0	-2.2	11	3	2	3.9	-5.1	-6	3	17	10.5	-2.9	3	4	5	14.8	-12.3	3	5	4	22.6	22.2
15	2	3	28.1	-22.4	-8	2	6	4.7	2.6	2	3	24	4.2	-1.2	11	3	2	3.9	-5.1	-6	3	19	22.2	-19.2	3	4	7	7.9	9.4	1	5	8	16.3	16.3
15	2	7	25.3	23.8	-8	2	8	5.2	8.9	2	3	1	4.6	-1.9	11	3	2	3.9	-5.1	-6	3	21	19.2	21.1	3	4	9	10.6	-9.2	1	5	10	26.9	-25.7
15	2	11	20.3	8.3	-8	2	12	31.7	-29.6	2	3	5	13.3	13.2	11	3	10	9.1	-3.6	-7	3	2	7.7	-8.5	3	4	13	25.8	-26.4	2	5	1	3.0	0.0
15	2	13	3.4	-6.5	-8	2	14	4.2	2.8	2	3	7	47.9	49.8	11	3	10	3.2	-5.1	-7	3	4	17.1	-20.2	4	4	0	9.3	-8.6	2	5	3	2.0	-0.2
15	2	15	21.0	-25.7	-8	2	16	22.6	-23.3	2	3	9	47.9	49.8	11	3	10	3.2	-5.1	-7	3	6	18.6	-48.6	4	4	5	21.7	-23.7	2	5	2	3.0	-0.2
15	2	17	12.0	-13.5	-8	2	18	25.3	-27.0	2	3	11	53.6	-55.1	12	3	3	14.4	19.0	-7	3	8	4.2	-0.5	4	4	6	37.1	-36.9	2	5	7	19.8	20.6
16	2	1	22.2	-20.7	-8	2	20	14.1	-16.6	2	3	13	7.6	-8.4	12	3	7	42.7	47.3	-7	3	10	11.2	8.3	4	4	6	3.7	8.8	2	5	9	17.1	15.6
16	2	3	4.6	6.3	-8	2	22	18.5	11.5	2	3	15	5.9	-1.7	12	3	7	42.7	47.3	-7	3	12	10.2	-10.2	4	4	8	25.0	-23.4	2	5	11	20.1	25.4
16	2	5	29.6	-26.5	-8	2	24	3.2	7.6	2	3	17	34.0	30.6	12	3	9	15.0	17.1	-7	3	14	33.1	-30.4	4	4	10	10.6	14.0	2	5	13	6.3	-4.5
16	2	7	17.0	22.0	-9	2	3	21.5	-21.7	2	3	19	46.7	43.1	12	3	11	15.0	-13.1	-7	3	16	34.7	-34.3	4	4	12	3.4	-5.5	3	5	0	16.1	-16.6
16	2	9	11.1	11.1	-9	2	5	42.7	-45.4	2	3	21	12.4	-19.9	12	3	13	15.0	17.4	-7	3	20	3.2	-5.3	5	4	1	9.1	7.3	3	5	4	7.4	-6.3
16	2	11	5.4	-6.3	-9	2	7	19.3	-20.3	2	3	23	19.1	-10.5	12	3	15	15.7	-12.4	-7	3	22	3.0	9.9	5	4	3	19.3	-17.3	3	5	6	6.4	-8.2
16	2	13	3.4	-6.7	-9	2	9	4.5	-6.0	2	3	25	42.2	-44.5	12	3	17	15.7	-12.4	-7	3	24	24.4	-19.9	5	4	5	11.0	-9.6	3	5	8	11.0	-9.4
17	2	1	11.3	-1.2	-9	2	11	5.2	9.2	3	3	2	53.4	-54.2	13	3	2	25.6	19.8	-8	3	3	13.0	-16.7	5	4	7	10.3	-10.5	3	5	10	25.7	-24.0
17	2	3	5.0	-1.6	-9	2	13	15.6	-17.8	3	3	4	17.2	-18.1	13	3	4	21.9	17.6	-8	3	5	33.3	-32.9	5	4	9	3.2	-6.2	3	5	9	16.5	17.6
17	2	5	23.0	-25.5	-9	2	15	17.3	17.7	3	3	6	25.7	-27.1	13	3	6	47.5	-45.2	-8	3	7	14.5	14.5	5	4	13	19.4	-18.4	4	5	3	17.0	16.8
17	2	7	11.5	-16.0	-9	2	17	18.3	-20.9	3	3	8	51.1	-51.6	13	3	8	30.4	-28.8	-8	3	9	10.0	-2.1	5	4	15	15.3	-15.3	4	5	4	15.3	17.7
17	2	9	3.4	9.5	-9	2	19	21.7	-23.5	3	3	10	54.9	-55.4	13	3	10	34.4	-32.8	-8	3	11	14.6	-14.6	5	4	17	2.5	-2.5	4	5	7	9.2	-8.5
18	2	1	3.4	9.5	-10	2	21	23.6	21.3	3	3	11	7.3	5.5	13	3	12	16.7	18.0	-8	3	13	11.7	12.8	6	4	4	3.0	6.8	4	5	9	9.1	-7.1
18	2	3	3.4	11.4	-10	2	23	24.6	34.1	3	3	12	17.4	20.0	13	3	14	16.0	18.0	-8	3	14	11.2	12.8	6	4	6	14.2	3.1	4	5	13	2.6	-5.0
18	2	5	31.2	13.8	-10	2	25	35.7	33.5	3	3	13	20.0	23.0	13	3	16	2.8	4.2	-8	3	15	3.2	2.5	6	4	10	17.9	16.6	5	5	0	6.7	-9.4
18	2	7	3.2	15.2	-10	2	27	14.2	-14.2	3	3	14	22.9	23.0	13	3	18	2.8	4.2	-8	3	16	3.2	2.5	6	4	12	6.5	-6.2	5	5	0	15.1	-15.1
18	2	9	3.2	15.2	-10	2	29	3.0	4.5	3	3	15	3.0	3.5	14	3	20	21.5	22.2	-8	3	17	15.1	15.1	7	4	1	9.0	9.3	5	5	4	8.9	8.9
18	2	11	11.3	-11.3	-10	2	31	11.8	11.8	4	3	1	40.1	41.7	14	3	2	10.2	10.6	-9	3	2	7.9	8.9	7	4	3	18.6	-18.0	5	5	6	3.3	6.1
18	2	13	9.7	-11.4	-10	2	33	9.5	-9.5	4	3	3	36.2	-35.2	14	3	4	11.7	12.4	-9	3	5	11.5	-11.5	7	4	5	11.5	-11.5	5	5	7	3.3	-2.5
18	2	15	7.4	-7.2	-10	2	35	17.3	-12.7	4	3	5	5.2	8.5	14	3	6	3.3	2.7	-9	3	6	8.6	-6.4	7	4	7	10.0	-10.3	5	5	10	10.4	-10.4
18	2	17	3.4	-3.4	-10	2	37	20.4	-19.5	4	3	7	20.4	-19.5	14	3	8	3.2	-3.2	-9	3	7	7.0	10.0	7	4	9	20.0	-21.1	5	5	12	14.3	-14.3
18	2	19	3.4	-3.4	-10	2	39	18.3	18.3	4	3	9	18.6	18.6	14	3	10	10.7	10.7	-9	3	8	6.5	-6.5	7	4	11	3.5	-3.5	5	5	13	16.4	-16.4
18	2	21	14.6	-14.6	-11	2	41	3.3	3.5	4	3	11	12.7	-11.4	14	3	12	12.3	-8.4	-9	3	14	29.1	-26.1	8	2	5	10.2	3.6	6	5	12	14.3	-14.3
18	2	23	14.6	-14.6	-11	2	43	16.2	-13.2	4	3	13	15.8	-15.2	15	3	2	11.6	11.4	-9	3	15	18.4	-18.4	8	2	7	6.5	-6.5	6	5	9	9.4	-9.4
18	2	25	14.6	-14.6	-11	2	45	18.0	-15.2	4	3	15	19.8	-15.2	15	3	4	12.3	-8.4	-9	3	16	13.4	9.9	8	2	9	10.2	3.6	6	5	10	12.4	-12.4
18	2	27	14.6	-14.6	-11	2	47	20.4	-17.2	4	3	17	21.6	-17.2	15	3	6	22.0	-21.2	-9	3	17	13.4	11.0	8	2	11	23.5	-23.5	6	5	11	12.2	-12.2
18	2	29	14.6	-14.6	-11	2	49	22.8	-19.2	4	3	19	23.8	-19.2	15	3	8	24.2	-24.2	-9	3	18	14.4	12.4	8	2	13	25.5	-25.5	6	5	12	14.0	-14.0
18	2	31	14.6	-14.6	-11	2	51	25.2	-21.2	4	3	21	26.0	-21.2	15	3	10	25.6	-25.6	-9	3	19	15.4	13.4	8	2	15	27.5	-27.5	6	5	13	15.8	-15.8
18	2	33	14.6	-14.6	-11	2	53	27.6	-23.2	4	3	23	28.2	-23.2	15	3	12	27.4	30.0	-10	3	20	16.4	14.4	8	2	17	29.5	-29.5	6	5	14	17.6	-17.6
18	2	35	14.6	-14.6	-11	2	55	30.0	-25.2	4	3	25	30.4	-25.2	15	3	14	29.2	31.8	-10	3	21	17.4	15.4	8	2	19	31.5	-31.5	6	5	15	19.4	-19.4
18	2	37	14.6	-14.6	-11	2	57	32.4	-27.2	4	3	27	32.6	-27.2	15	3	16	31.0	34.4	-10	3	22	18.4	16.4	8	2	21	33.5	-33.5	6	5	16	21.2	-21.2
18	2	39	14.6	-14.6	-11	2	59	34.8	-29.2	4	3	29	34.8	-29.2	15	3	18</																	



In fact, computing the quantity of  $\text{Mn}^{4+}$  ( $= x$ ) from grand octahedral averages gives  $x = [(d_{\text{Mg}^{2+}-\text{O}}) - (d_{\text{Mg}^{(3)-\text{O}}})] / [(d_{\text{Mg}^{2+}-\text{O}}) - (d_{\text{Mn}^{4+}-\text{O}})] = (2.08 - 2.05) / (2.08 - 1.94) = 0.21$  where  $d_{\text{Mn}^{4+}-\text{O}}$  obtains from the tables of Shannon and Prewitt (1969). In the structure of warwickite, we shall confirm the solid solution ( $\text{Mg}^{2+}$ ,  $\text{Ti}^{4+}$ ) over a set of equivalent sites which supports the existence of ( $\text{Me}^{2+}$ ,  $\text{Me}^{4+}$ ) solutions in such compounds.

The octahedral O-O' edge distances and O-Me-O' angles obtain from (1) the geometry arising from the Jahn-Teller distortion of  $\text{Mn}^{3+}$ , (2) the existence of shared edges with no symmetry constraints, and (3) the existence of symmetry-constrained shared edges. In general, we shall analyze the polyhedral distortions by examining the following regions: (a) the shared O-O' equatorial edges for  $\text{Mn}^{3+}$ ; (b) the shared remaining edges, or the "elongate edges" for  $\text{Mn}^{3+}$ ; (c) the edges constrained by the fiber repeat, that is those shared edges parallel to the fiber axis.

Of these three kinds of shared edges, we find the third most interesting for all three structures, for it is these fiber-repeat edge distances which seemingly violate the expected electrostatic distortions owing to the constraints of the repeat distance.

Table 6a lists the Mn-O, Mg-O, and B-O polyhedral distances in ascending values. We would expect shared edges between  $\text{Mn}^{3+}$ - $\text{Mn}^{3+}$  (equatorial)

FIG. 1. (a) Idealized arrangement of octahedral columns (ruled) and  $\text{BO}_3$  triangles (stippled) mapped on the triangular tessellation for hulsite. (b) Idealized arrangement for warwickite. (c) Idealized arrangement for wightmanite from Moore and Araki (1972).

$< \text{Mn}^{3+}(\text{equatorial})-\text{Mg}^{2+} < \text{Mn}^{3+}(\text{elongate edges})-\text{Mg}^{2+} < \text{Mg}^{2+}-\text{Mg}^{2+}$ . The O-Me-O' angles associated with the O-O' edges increase accordingly, with the most severe distortions taken up by the "soft" Mg-O polyhedra as a consequence of  $\text{Mn}^{3+}-\text{Mg}^{2+}$  repulsions. This, in fact, is what we observe, except for

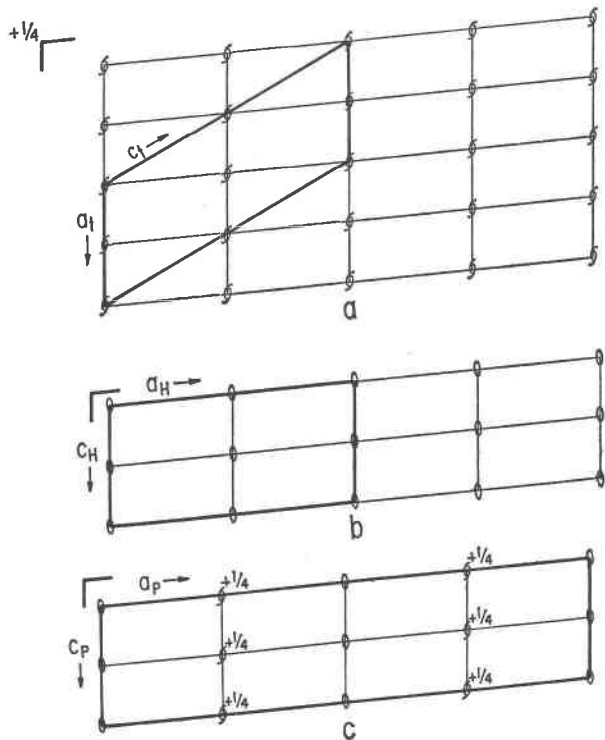


FIG. 2. Diagrams showing symmetry elements and cell outlines (drawn bold) for pinakiolite and hulsite. Inversion centers occur at the origins and centers of the cells. (a) The cell of Takéuchi, Watanabe, and Ito (1950), with axes  $a_T$  and  $c_T$ . (b) The cell of hulsite, with axes  $a_H$  and  $c_H$ . (c) The cell of pinakiolite, with axes  $a_P$  and  $c_P$ .

the fiber repeat distances  $O(7)$ - $O(7)'$  associated with  $Mg(1)$  and  $Mg(2)$ . The fiber repeat distances, as Table 6a indicates, are the longest edges for their polyhedra. In part, these long shared edges arise from the shortening of the edge-sharing  $Mn^{3+}$  octahedra along the fiber direction. More important, however, is the geometry of the cations about  $O(7)$ : five octahedral centers coordinate to this anion, de-

fining an octahedraon of cations with one missing vertex. As we shall discuss under wightmanite, such a configuration of cations about an anion results in three-dimensional cation-cation repulsion effects with a lengthening of a shared edge greater than the value expected when the cationic repulsions are confined to a line.

### Electrostatic Basis for the Pinakiolite Ordering Scheme

The ordering scheme for pinakiolite can be explained from the electrostatic valence balances (e.v.b.'s) of anions in Table 7a. The lengthened  $Mn^{3+}$ -O apical distances are in the plane perpendicular to the  $y$ -direction. Treating the e.v.b.'s on the basis of regular octahedra, it is seen that  $O(1)$ ,  $O(2)$ ,  $O(3)$ , and  $O(6)$  are oversaturated by  $\Delta\Sigma = +0.17$  e.s.u. These each include one  $Mn^{3+}$ -O apical bond. The undersaturated oxygen,  $O(8)$  with  $\Delta\Sigma = -0.34$  e.s.u., includes two  $Mn^{3+}$ -O equatorial bonds. The Jahn-Teller distortion leads, electrostatically, to weaker-than-average bond strengths in the apical direction and stronger-than-average bond strengths in the equatorial direction.  $O(7)$ , which is "neutral," includes two  $Mn^{3+}$ -O equatorial and three  $Mg$ -O bonds. According to the electrostatic model advanced for the Jahn-Teller distortion and its effect on bond strengths, the  $Me$ - $O(7)$  distances should be longer than average. Indeed,  $Mg(1)$ ,  $Mg(2)$ , and  $Mg(4)$  all provide longer- than-average distances to  $O(7)$ .  $Mg(4)$ , which is fully occupied and therefore not "expanded" owing to partial occupancy, possesses a long  $Mg(4)$ - $O(7)$  2.16 Å distance.

Another interesting feature of the structure is that the ordering scheme leads to a  $C$ -centered structure with doubled  $a$ - and  $b$ -axes relative to the  $P$ -cell of hulsite. Why aren't the  $Mn(1)$  and  $Mn(2)$  atoms distributed along the same level on  $y$  throughout, so

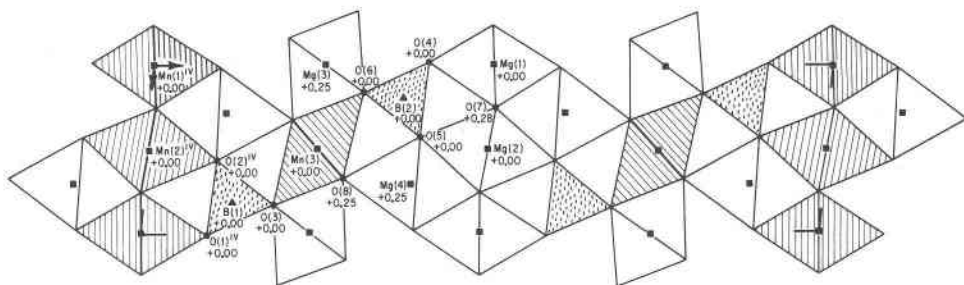


FIG. 3. (a) Polyhedral diagram of the real pinakiolite structure between  $O \leq y \leq 1/2$ .  $Mn^{3+}$ -O octahedra are ruled,  $Mg$ -O octahedra are unshaded, B-O triangles are stippled. Atomic positions are labelled to correspond with Table 4a.

that pinakiolite remains  $P2/m$  but with the  $b$ -axis of hulsite doubled? This appears as a consequence of the severe geometrical distortion that would result if all  $Mn^{3+}$  cations were on one level along  $y$  and all the  $Mg^{2+}$  cations on the level  $y + 1/2$ . Slabs normal to the  $y$ -direction would alternately bulge and shrink. In other words, ordering along the  $a$ -direction minimizes strain in the crystal.

From this discussion, two arguments are advanced toward prediction of the ordered structure of  $Mg^{2+}Mn^{3+}$ -equivalents of  $Mg^{2+}Fe^{3+}$ -bearing borates.

1.  $Mn^{3+}$  occupies those sites where electrostatically oversaturated anions (referring to the isotropic octahedron) are associated with  $Mn^{3+}$ -O apical bonds and undersaturated anions with  $Mn^{3+}$ -O equatorial bonds.
2. Successive bands of octahedra contain alternate  $Mn^{3+}$ -O layers and  $Mg^{2+}$ -O layers to minimize geometrical distortion.

Can this problem be applied to the ludwigite-orthopinakiolite relationship? Ludwigite,  $Mg_2Fe^{3+}O_2[BO_3]$ ,  $Pbam$  (with  $c$  the fiber direction), was studied by Takéuchi, Watanabe, and Ito (1950). The  $Mn^{3+}$ -analogue, orthopinakiolite,  $Pnmm$  (with  $b$  and  $c$  of

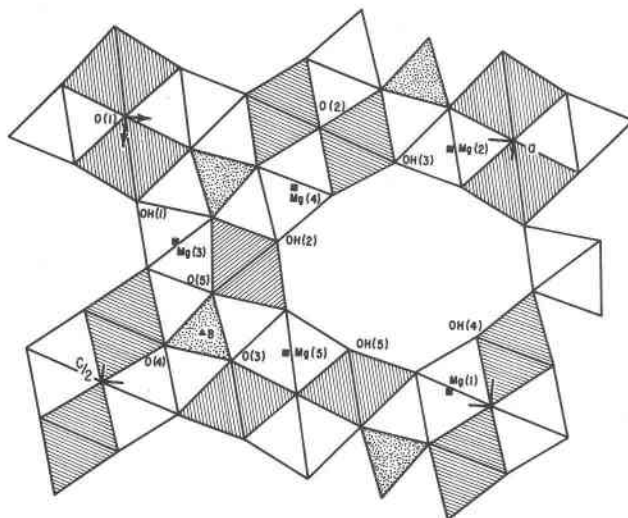


FIG. 3(c). Polyhedral diagram of the real wightmanite structure from Moore and Araki (1972). Octahedra at  $y = 0$  are unshaded, octahedra at  $y = 1/2$  are ruled. The B-O triangles are stippled.

the ludwigite cell doubled), was investigated in a preliminary study by Randmets (1960). The curious feature of the orthopinakiolite cell is that ordered arrangements based on ludwigite can be found which give space group  $Pnmm$  but which *do not* require a doubled  $b$ -axis. In other words  $Pnmm$  can be obtained from  $Pbam$  by doubling  $c$  but cannot be derived by doubling  $b$ . For this reason, we feel that orthopinakiolite may show a different topology than ludwigite and a study on its structure is in progress.

### Warwickite

#### Experimental

Several years ago, P.B.M. collected specimens of warwickite-forsterite-spinel-chondrodite nodules embedded in coarsely crystallized marble from the type locality near Amity, about seven miles from Warwick, Orange County, New York. Accessory minerals include pyrrhotite, dravite, sphene, magnetite, and flecks of graphite. The warwickite occurs as rough black prisms.

The crystal, a symmetrical prism  $0.21 \times 0.15 \times 0.35$  mm in dimension was rotated about the  $c$ -axis on a PAILRED automated diffractometer using  $MoK\alpha$  radiation and graphite monochromator. Data were collected to  $2\theta = 70^\circ$  for the  $l = 0$ - to 4- levels. Polyhedral absorption correction was applied utilizing the Gaussian integral method of Burnham (1966) and symmetry equivalent reflections were

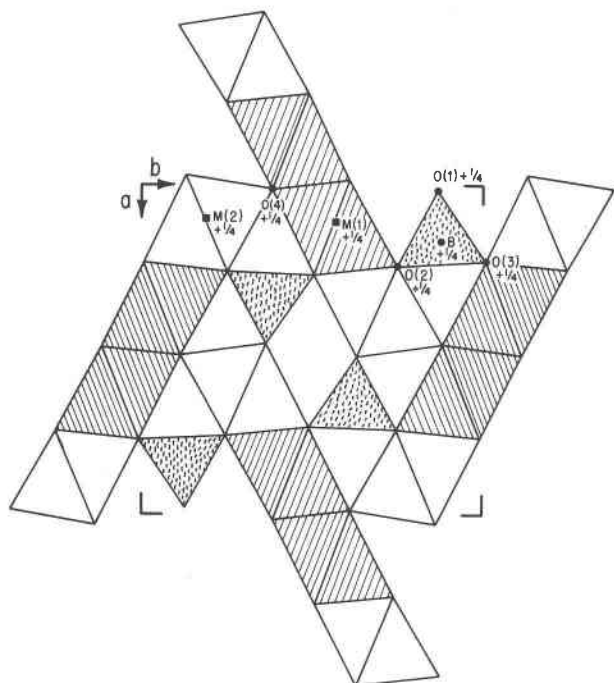


FIG. 3(b). Polyhedral diagram of the real warwickite structure. The (Mg,Ti)-O octahedra are ruled, Mg-O octahedra are unshaded, B-O triangles are stippled. Atomic positions are labelled to correspond with Table 4b.



TABLE 6c. Wightmanite. Polyhedral Interatomic Distances and Angles\*  
(Estimated standard errors in distances less than 0.01 Å)

A-region of bundle													
Mg(1)			Mg(5)			Mg(3)							
1	Mg(1)	-OH(4)	2.02	Å	1	Mg(5)	-OH(5)	2.00		2	Mg(3)	-OH(2)	2.03
2		-OH(3)	2.03		2		-OH(1)	2.04		1		-OH(1)	2.04
1		-O(4)	2.07		1		-O(3)	2.05		1		-O(5)	2.11
2		-O(2)	2.17		2		-O(1)	2.17		2		-O(5)	2.13
average			2.08	Å	average			2.08		average			2.08
O-Me-O'													
2	O(2)	ii	-OH(3)	ii	2.83 <sup>a</sup>	84.66 <sup>o</sup>	2	O(1)	ii	-OH(1)	ii	2.84 <sup>a</sup>	84.78
2	O(2)	ii	-OH(4)	ii	2.84 <sup>a</sup>	85.27	2	O(1)	ii	-OH(5)	ii	2.83 <sup>a</sup>	85.38
2	OH(4)	ii	-OH(3)	ii	2.90	91.46	2	OH(5)	ii	-OH(1)	ii	2.90	91.75
2	OH(3)	ii	-O(4)	i	2.98	93.24	2	OH(1)	ii	-O(3)	i	2.97	93.13
2	O(2)	ii	-O(4)	i	2.99 <sup>a</sup>	89.66	2	O(1)	ii	-O(3)	ii	2.97 <sup>a</sup>	89.42
1	O(2)	ii	-O(2)	ii	3.10 <sup>a</sup>	91.17	1	O(1)	ii	-O(1)	ii	3.10 <sup>a</sup>	91.17
1	OH(3)	ii	-OH(3)	ii	3.10	99.56	1	OH(1)	ii	-OH(1)	ii	3.10	98.90
average			2.94		89.94		average			2.94		89.92	
B-region of bundle													
Mg(2)			Mg(4)			B							
1	Mg(2)	-OH(3)	2.03		1	Mg(4)	-OH(2)	1.99		1	B	-O(3)	1.38
2		-OH(5)	2.04		2		-OH(4)	2.04		1		-O(4)	1.38
2		-O(3)	2.13		2		-O(4)	2.12		1		-O(5)	1.39
1		-O(1)	2.17		1		-O(2)	2.18		average			1.38
average			2.09		average			2.08		1	O(3)	-O(4)	2.38
2	OH(5)	ii	-O(3)	ii	2.78 <sup>a</sup>	83.59	2	OH(4)	ii	-O(4)	ii	2.77 <sup>a</sup>	83.48
2	O(1)	ii	-OH(5)	ii	2.83 <sup>a</sup>	84.42	2	O(2)	ii	-OH(4)	ii	2.83 <sup>a</sup>	84.16
2	OH(3)	ii	-OH(5)	ii	2.94	92.50	2	OH(2)	ii	-OH(4)	ii	2.92	92.85
2	O(1)	ii	-O(3)	ii	2.97 <sup>a</sup>	87.37	2	O(2)	ii	-O(4)	ii	2.99 <sup>a</sup>	88.10
2	O(3)	iii	-OH(3)	iii	3.10	96.32	2	O(4)	ii	-OH(2)	ii	3.03	94.94
1	OH(5)	ii	-OH(5)	ii	3.10	98.90	1	OH(4)	ii	-OH(4)	ii	3.10	98.90
1	O(3)	iii	-O(3)	iii	3.10	93.39	1	O(4)	ii	-O(4)	ii	3.10	93.96
average			2.95		90.06		average			2.94		90.00	
1	O(3)	iii	-O(5)	iii	3.10	119.16 <sup>o</sup>							
1	O(4)	iii	-O(5)	iii	2.40	120.09							
1	O(3)	iii	-O(5)	iii	2.40	120.09							
average			2.39		119.78								

\* i = -x, -y, -z; ii = 1/2-x, 1/2+y, 1/2-z; iii = 1/2+x, 1/2+y, 1/2+z; t = 1+y applied to coordinates in Moore and Araki (1972).

<sup>a</sup>Shared edges between Mg-O octahedra.

averaged. Unobserved reflections less than 2σ(I) were set to I(hkl) = σ(I). The |F(obs)| were weighted on the basis of counting statistics and error in crystal size measurement. All reflections were used in the structure determination and refinement.

Refined structure cell parameters were obtained from an indexed diffractometer trace using CuKα radiation, Si(a = 5.4301 Å) as an internal standard, and a scan rate of 0.5°/minute. The results are given in Table 2b.

TABLE 7a. Pinakiolite. Electrostatic Valence Balances of Cations about Anions\*

Anions	Coordinating Cations	Bond Strengths	ΔΣ	Comments
O(1)	B(1)+Mn(1)+2Mg(4)	3/3+2/6+2/6+2/6	+ 1/6	Mn <sup>3+</sup> apical
O(2)	B(1)+Mn(2)+2Mg(4)	3/3+3/6+2/6+2/6	+ 1/6	Mn <sup>3+</sup> apical
O(3)	B(1)+Mn(3)+2Mg(3)	3/3+3/6+2/6+2/6	+ 1/6	Mn <sup>3+</sup> apical
O(4)	B(2)+Mg(1)+2Mg(4)	3/3+2/6+2/6+2/6	+ 0	No Mn <sup>3+</sup>
O(5)	B(2)+Mg(2)+2Mg(4)	3/3+2/6+2/6+2/6	+ 0	No Mn <sup>3+</sup>
O(6)	B(2)+Mn(3)+2Mg(3)	3/3+3/6+2/6+2/6	+ 1/6	Mn <sup>3+</sup> apical
O(7)	Mn(1)+Mn(2)+Mg(1)+Mg(2)+Mg(4)	3/6+3/6+2/6+2/6+2/6	+ 0	Mn <sup>3+</sup> square plane
O(8)	2Mn(3)+Mg(3)+Mg(4)	3/6+3/6+2/6+2/6	- 2/6	Mn <sup>3+</sup> square plane

\*Based on ideal composition Mn(1)=Mn(2)=Mn(3) = Mn<sup>3+</sup>; Mg(1)=Mg(2)=Mg(3)=Mg(4) = Mg<sup>2+</sup>.

TABLE 7b. Warwickite. Electrostatic Valence Balances of Cations about Anions\*

Anion	Coordinating Cations	Bond Strengths	$\Sigma$	$\Delta\Sigma$	Comments
0(1)	B+2M(2)	$3/3+.83(2/6)(2)+.17(3/6)(2)$	1.73	-0.27	B-0(1), M(2)-0(1) short
0(2)	B+M(1)+2M(2)	$3/3+.53(2/6)+.13(3/6)+.34(4/6)+.83(2/6)(2)+.17(3/6)(2)$	2.19	+0.19	B-0(2) average; M(1)-, M(2)-0(2) long
0(3)	B+2M(1)+M(2)	$3/3+.53(2/6)(2)+.13(3/6)(2)+.34(4/6)(2)+.83(2/6)+.17(3/6)$	2.30	+0.30	B-0(3) average; M(1)-, M(2)-0(3) long
0(4)	3M(1)+M(2)	$.53(2/6)(3)+.13(3/6)(3)+.34(4/6)(3)+.83(2/6)+.17(3/6)$	1.78	-0.22	M(1)-, M(2)-0(4) short
$\text{Co}^{2+}\text{Fe}^{3+}\text{O}[\text{BO}_3]$					
$\Delta\Sigma$ about M(1)=Fe <sup>3+</sup> :		$\Delta\Sigma(0(2)) + 2\Delta\Sigma(0(3)) + 3\Delta\Sigma(0(4))$	$1/6+4/6-3/6 = +0.33$		
" about M(2)=Co <sup>2+</sup> :		$2\Delta\Sigma(0(1)) + 2\Delta\Sigma(0(2)) + \Delta\Sigma(0(3)) + \Delta\Sigma(0(4))$	$-4/6+2/6+2/6-1/6 = -0.17$		
Warwickite					
$\Delta\Sigma$ about M(1)			$0.19+2(0.30)+3(-0.22) = +0.13$		
" about M(2)			$2(-0.27)+2(0.19)+0.30-0.22 = -0.08$		
* Bond strengths computed from proposed site distributions. M(1) = 0.53 Mg <sup>2+</sup> + 0.09 Al <sup>3+</sup> + 0.04 Fe <sup>3+</sup> + 0.34 Ti <sup>4+</sup> and M(2) = 0.83 Mg <sup>2+</sup> + 0.08 Al <sup>3+</sup> + 0.09 Fe <sup>3+</sup> .					

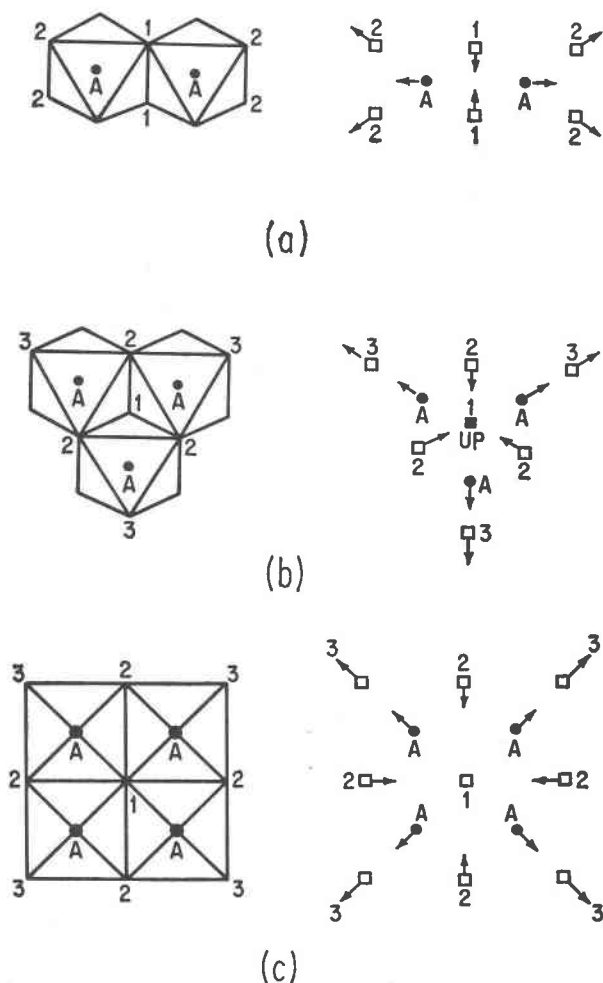


FIG. 4. Vector diagrams of cation-cation repulsions for the octahedral dimer (a), trimer (b), and tetramer (c). Centers and vertices of perfect octahedra are labelled on the left to correspond with the resultants on the right.

### Structure Determination and Refinement

The unit formula of warwickite is approximately  $\text{Mg}^{2+}_{1.33}\text{Al}^{3+}_{0.21}\text{Fe}^{3+}_{0.12}\text{Ti}^{4+}_{0.34}\text{O}[\text{BO}_3]$  of which the octahedral cations must be distributed over two independent sites, M(1) and M(2), each of equipoint rank number 4.

Vector set analysis of the  $P(uvw)$  map provided a minimum function  $M_4(xyz)$  which included all octahedral cations and two oxygen atoms. The  $\gamma'$ -synthesis revealed all remaining atoms in the structure. Scattering curves include Mg<sup>2+</sup>, Ti<sup>4+</sup>, and O<sup>1-</sup> from the tables of Cromer and Mann (1968) and B<sup>1+</sup> from Onken and Fischer (1968). Anomalous dispersion effects were applied to Ti<sup>4+</sup> and Mg<sup>2+</sup>. Refinement proceeded from several models: the distribution  $M(1) = \text{Mg}^{2+}$ ,  $M(2) = 0.5 \text{Ti}^{4+} + 0.5 \text{Mg}^{2+}$ ;  $M(1) = 0.5 \text{Ti}^{4+} + 0.5 \text{Mg}^{2+}$ ,  $M(2) = \text{Mg}^{2+}$ ; and  $M(1) = 0.25 \text{Ti}^{4+} + 0.75 \text{Mg}^{2+}$ ,  $M(2) = 0.25 \text{Ti}^{4+} + 0.75 \text{Mg}^{2+}$ . The scattering distributions were then allowed to vary. Convergence, including all 652 non-equivalent reflections, led to the  $R(hkl)$  distribution in Table 3b. The favored distribution is  $M(1) = \text{Mg}_{0.62}\text{Ti}_{0.38}$  and  $M(2) = \text{Mg}_{0.96}\text{Ti}_{0.04}$ , suggesting the ideal formula  $\text{Mg}(\text{Mg}_{0.5}\text{Ti}_{0.5})\text{O}_2[\text{BO}_3]$ . The final atomic coordinates and isotropic thermal vibration parameters appear in Table 4b, and the structure factor data are given in Table 5b.

Since the Ti<sup>4+</sup> and Fe<sup>3+</sup> and Mg<sup>2+</sup> and Al<sup>3+</sup> scattering profiles are similar, it is not possible to distinguish them with any certainty, at least for the minor concentrations of Fe<sup>3+</sup> and Al<sup>3+</sup> in the crystal. We propose  $M(1) = \text{Mg}^{2+}_{0.50}\text{Al}^{3+}_{0.12}\text{Ti}^{4+}_{0.34}\text{Fe}^{3+}_{0.04}$  and  $M(2) = \text{Mg}^{2+}_{0.83}\text{Al}^{3+}_{0.09}\text{Fe}^{3+}_{0.08}$  based on the scattering densities and the interatomic distance averages. Naturally, the correct distribution for Fe<sup>3+</sup> cannot

be ascertained except through some independent study such as a Mössbauer resonance experiment.

### Topology of the Structure

Warwickite (Fig. 1b) consists of bands of edge-sharing octahedra, four octahedra wide, oriented parallel to {210}. Although the structure for warwickite proposed by Takéuchi, Watanabe, and Ito (1950) is confirmed, the present more complete data set allowed a more reliable assessment of site occupancies. A polyhedral diagram of the actual structure is presented in Figure 3b.

During this study, the refinement of the isotype,  $\text{Co}^{2+}\text{Fe}^{3+}\text{O}[\text{BO}_3]$  by Venkatakrisnan and Buerger (1972) was brought to our attention. Their proposed site distribution  $M(1) = \text{Me}^{3+}$  and  $M(2) = \text{Me}^{2+}$  on the basis of an observed difference in electron density distribution agrees with our conclusion that warwickite has essentially all of its  $\text{Ti}^{4+}$  in the  $M(1)$  site with  $(\text{Mg}_{0.5}\text{Ti}_{0.5})$  as the probable limit. They concluded, on the basis of electrostatic valence sums for  $M(1) = \text{Me}^{3+}$  that this model affords the minimum average deviation. In Table 7b, we provide electrostatic valence sums of cations about anions with comments on the bond distances to the individual anions and note further support of this argument.

### Interatomic Distances

Polyhedral interatomic distances, angles, and their averages appear in Table 6b along with the data for  $\text{Co}^{2+}\text{Fe}^{3+}\text{O}[\text{BO}_3]$ . As with  $\text{Co}^{2+}\text{Fe}^{3+}\text{O}[\text{BO}_3]$ , the average distances for the  $M(1)$ - and  $M(2)$ -O octahedra are very similar. Differences in distances between warwickite and  $\text{Co}^{2+}\text{Fe}^{3+}\text{O}[\text{BO}_3]$  are small, with averages about 0.02 Å greater for the octahedra in the latter compound. In both structures, the shared edges are the shortest for their polyhedra.

From the tables of Shannon and Prewitt (1969), we have estimated the average distances,  $M(1)$ -O 2.06 Å and  $M(2)$ -O 2.08 Å based on the sums of the ionic radii of the constituents we propose to be present in warwickite. For  ${}^{\text{vi}}\text{Fe}^{3+}\text{-ivO}$  and  ${}^{\text{vi}}\text{Co}^{2+}\text{-ivO}$ , these values are approximately 2.03 and 2.10 Å respectively. Then why are the average  $M(1)$ -O and  $M(2)$ -O distances in the  $\text{Co}^{2+}\text{Fe}^{3+}\text{O}[\text{BO}_3]$  structure almost identical? We propose that this is an effect of overall electrostatic deviations from neutrality. For the anions of the  $\text{Co}^{2+}$ -O octahedron, the deviation sum is  $-1/6$  e.s.u. and, for the  $\text{Fe}^{3+}$ -O octahedron, the deviation sum is  $+2/6$  e.s.u. The result

is an  $\text{Co}^{2+}$ -O average shorter than, and an  $\text{Fe}^{3+}$ -O average longer than, the averages found in structures with locally neutral valence balances about the polyhedra. We note that the same calculations for warwickite result in a deviation sum of  $+0.13$  e.s.u. about  $M(1)$  and  $-0.08$  e.s.u. about  $M(2)$ , so that this effect is much smaller, resulting in closer agreement of interatomic averages with those predicted. For a mixed crystal with  $\text{Me}^{2+}$ ,  $\text{Me}^{3+}$ , and  $\text{Me}^{4+}$  cations, the preferential site occupancies evidently minimize such polyhedral deviation sums as well as minimizing the individual deviations about each anion.

## Wightmanite

### Experimental

The crystal structure of wightmanite was reported by Moore and Araki (1972). We provide here the bond distance and bond angle data of this extraordinary structure. The details of the data collection follow from the pinakiolite study except that absorption correction was not necessary. (An error appears in the earlier paper: the data were collected on a PAILED automated diffractometer.) Cell parameters are  $a$  13.46(2) Å,  $b$  3.102(5),  $c$  18.17(2),  $\beta$  91.60(5)°,  $I2/m$ , with the errors estimated from  $\omega$ -scans about the  $b$ -axis. The formula is  $\text{Mg}^{2+}_5(\text{O})(\text{OH})_5[\text{BO}_3] \cdot n\text{H}_2\text{O}$  ( $n_{\text{max}} = 2$ ), of which there are four formula units in the cell. The analysis in Murdoch (1962)—which is essentially that of a rather pure basic magnesium borate hydrate with small amounts (<3 percent each) of  $\text{CaO}$ ,  $\text{FeO}$  and  $\text{Al}_2\text{O}_3$ —seems satisfactory. The  $R(hkl)$  dependence on  $|F(hkl)|$  magnitudes is listed in Table 3c.

### Structure Topology

Figure 1c presents the mapping of octahedra and triangles upon the triangular tessellation, and Figure 3c presents a sketch of the actual structure distortions along with locations of the atomic positions. The structure is locally electrostatically neutral with respect to the distribution of cations about anions when the hydrogen bonds are not considered. Owing to the disorder in the channels, we have not located the hydrogen atoms. We do not reproduce the atomic coordinate parameters since they appear in the earlier paper, but the structure factor data appear in Table 5c. To further appreciate the framework character of the structure, the anisotropic thermal vibration parameters appear in Table 4c; it is clear

that the ellipsoids do not deviate greatly from spherical shape for the framework portion of the structure.

The wightmanite structure is an octahedral framework structure, built of octahedral bundles and bands two octahedra in width. Two sets of non-equivalent bundles occur in the structure, and they possess identical structure topology. Enormous channels occur in the structure and these are occupied by disordered water molecules.

#### Bond Distances and Angles

The octahedral bundles in wightmanite can be conceived as fibrous fragments of the periclase (*i.e.*, rocksalt) structure. Six octahedral centers in a bundle coordinate to an oxide ( $O^{2-}$ ) anion. A similar arrangement was discovered by Moore (1969) in the crystal structure of gageite, the octahedral framework of which is  $(Mn,Mg)^{2+}_7(O)(OH)_{12}$ . In heptasodium fluoride-bisarsenate-19-hydrate,  $[Na_6F(H_2O)_{18}][Na(H_2O)(AsO_4)_2]$ , six  $Na^+$  cations octahedrally coordinate to one  $F^-$  defining an octahedral hexamer topologically isomorphous with  $[Ta_6O_{19}]^{8-}$  and  $[Nb_6O_{19}]^{8-}$  (Tillmanns and Baur, 1970). All these structures possess one central anion whose nearest neighbor cations are isomorphous to the cation neighborhood of the rocksalt structure. The wightmanite structure provides stimulus for a detailed discussion on local polyhedral distortions in this fragmented periclase structure.

Table 6c provides the interatomic distances and angles for wightmanite. The Mg(1) and Mg(5) and the Mg(2) and Mg(4) polyhedral distances are conveniently listed in pairs, since these are the topologically matched regions in the two symmetrically non-equivalent bundles. The "A" region consists of the octahedra which share an edge parallel to the fiber direction and which contribute four coplanar bonds to the oxide anion; and the "B" region consists of the remaining octahedra which contribute two apical bonds to the oxide anion. The Mg-O, O-O', and O-Mg-O' distances and angles match close to their limits of error for Mg(1) and Mg(5) and for Mg(2) and Mg(4). In discussion of bond distances this adds support to arguments based on cation-cation repulsion effects when making comparisons between crystals as well as within a crystal. All distances to the central oxide anion are long (Mg-O 2.17–2.18 Å) while those to the apical corner-sharing vertices are short (Mg-O 1.99–2.03 Å). We conclude that, in the progressive condensation of octa-

hedra by edge-sharing, the aggregate expands in the interior and shrinks around the periphery. The increase in anion radius with increase in coordination number of cations about the anion has been reviewed in detail by Shannon and Prewitt (1969).

The dilation in distance of cations about the central anion, however, is a much more profound effect than earlier anticipated. For example, O(1) and O(2) in wightmanite can be written  ${}^{vi}Mg$ - ${}^{vi}O$  with average distance of 2.17 Å, yet  ${}^{vi}Mg$ - ${}^{vi}O$  in periclase is 2.105 Å. In gageite,  ${}^{vi}Mn$ - ${}^{vi}O$  has an average distance of 2.29 Å while that in manganosite is 2.22 Å. In  $[Na_6F(H_2O)_{18}]^{5+}$ , the  ${}^{vi}Na$ - ${}^{vi}F$  distance is 2.42 Å, but  ${}^{vi}Na$ - ${}^{vi}F$  is 2.31 Å in villiamite, NaF. Since these dilations of at least 0.05 Å compared with the rocksalt structures are in the range of maximal anion radii differences suggested by Shannon and Prewitt (1969), who state  $r({}^{vi}O^{2-}) - r({}^{ii}O^{2-}) = 0.05$  Å, it appears that structure topology has a profound effect in average polyhedral distances as well as the anion coordination by cations.

This severe Me-anion distance dilation probably results from cation-cation repulsion effects. A sketch of various anion-cation configurations based on polynuclear octahedral clusters is featured in Figure 4. The classical model states that cations, when brought together, move away from each other along their lines of force across a shared edge and, to conserve the Me-anion distances, the anions on the shared edge move toward each other. For the edge dimer, the peripheral anions "ride" with the cations along their lines of coulombic repulsion. In the octahedral trimer, the central anion moves up or down normal to the plane to conserve the Me- $\varphi$  distance. However, in the octahedral tetramer, the central anion is constrained to remain in the plane of the circumjacent cations. Accordingly, its Me- $\varphi$  distance should be longer than average. Finally, in the hexamer,  $M_{6\varphi 19}$ , all six cations move away from the central anion. The pentameric arrangement would also show this effect, but less profound owing to its non-centric structure and some "riding" motion of the central oxide anion. In all these structures, the apical or terminal anions ride along with the cations in the direction of the net lines of cation-cation repulsion. The result is that the  $M_{6\varphi 19}$  cluster bulges in the center.

Then why do these clusters shrink at the periphery? The answer appears to lie in anion undersaturation. Evans (1971), in his extensive review of the isopolyanion clusters such as  $[V_{10}O_{28}]^{9-}$ ,  $[Nb_6O_{19}]^{8-}$ ,

$[\text{Mo}_7\text{O}_{24}]^{6-}$ , etc, notes that all terminal oxide anions have short Me-O<sup>2-</sup> distances since they coordinate to only one cation and are severely undersaturated. In wightmanite, the terminal anions involve OH-ligands which receive three Mg<sup>2+</sup> bonds. According to Baur (1970),  $\Delta\Sigma = -1/6$  for the oxygen associated with the hydroxyl bonded to three Mg<sup>2+</sup> cations on account of the O-H...O hydrogen bond. Consequently, the Mg-OH distances are shorter than average, as observed for all such bonds in wightmanite. Despite these severe distortions, the average Mg-O distances for each octahedron of 2.08-2.09 Å are the expected averages for mean <sup>vi</sup>Mg-<sup>iii</sup>O, conforming with Rule 3 of Baur (1970).

It is now clear why the octahedral bundle is particularly stable in crystals involving the same cations (such as Mg<sup>2+</sup>) and anions (such as O<sup>2-</sup>) and why edge sharing parallel to the fiber repeat other than in a bundle would be unstable for these crystals. For a bundle, dilation of the core Me-O<sup>2-</sup> distances assures the same fiber axis repeat as found for the octahedra whose edges parallel to the fiber direction are not shared. For other arrangements, the shared edge would be shortened (compare with the edge-sharing dimer) and a misfit between shared and unshared edges parallel to the fiber repeat would occur. For this reason, it is predicted that arrangements with larger cross-sections would be unstable in 3 Å fiber structures since, by adding a further neighborhood of cations, the dilation at the anion core would diminish slightly and a mismatch between shared and unshared edges along the fiber direction would occur. This arises because cation-cation repulsions will be *toward* the central anion as well as *away* from it. We stress this point since it is clear that tables of ionic radii may lead to erroneous predictions in interatomic averages for certain structure topologies, in particular the tetramer, pentamer, and the hexamer depicted here.

### Concluding Remarks About the Wallpaper Structures

The investigation of three different wallpaper structures permits us to draw conclusions and offer predictions about this family of compounds.

#### Ordering of Cations of Mixed Charge: Derivative Structures

Site distributions of cations of similar radius but different charge proceed from an ideal structure type—the triangular net—to that arrangement which

minimizes deviations from perfect electrostatic valence sums. Distortions of the polyhedra, including the Me-O distances, conform with the order of the deviations. The solid solution of cations with similar radius but grossly different charge, such as Me<sup>2+</sup> and Me<sup>4+</sup>, occurs if it leads to a minimum deviation in valence sums. Thus, the warwickite structure provides in the limit  $M(1) = \text{Me}_{0.5}^{2+} + \text{Me}_{0.5}^{4+}$  and  $M(2) = \text{Me}^{2+}$ . By analogy, we would propose that other warwickites may exist such as  $\text{Mg}(\text{Mg}_{0.5}\text{Sn}_{0.5}^{4+})\text{O}[\text{BO}_3]$  and  $\text{Mg}(\text{Mg}_{0.5}\text{Mn}_{0.5}^{4+})\text{O}[\text{BO}_3]$ , the latter suggested by the partial replacement of Mg<sup>2+</sup> by Mn<sup>4+</sup> in the Mg(3) site of pinakiolite.

The substitution of electronically anisotropic cations such as Mn<sup>3+</sup> proceeds to a derivative structure since Me<sup>2+</sup>-Mn<sup>3+</sup> solid solution does not occur and results in a derivative cell. Again, the ordering scheme provides the space group which affords minima in deviations from electrostatic balance of cations about anions.

#### Edge-Sharing Parallel to the Fiber Axis

One of the limitations inherent in the 3 Å wallpaper structures is the common fiber axis repeat for all non-equivalent octahedra in any structure. Serious mismatches in octahedral edge-distances would require local oxygen disorder in the framework and severe anisotropy of the mean residence ellipsoids, with the axis of elongation or compression parallel to the fiber direction. Disordered tetrahedral groups resulting from serious mismatches between tetrahedral edge and octahedral edge distances parallel to the fiber axis have been noted in the structures of gageite (Moore, 1969) and chlorophoenicite,  $\text{Mn}^{2+}_3\text{Zn}_2(\text{OH})_6[\text{As}_{0.5}\text{H}_{0.5}](\text{O},\text{OH})_3]_2$  (Moore, 1968). These structures, however, possess rigid octahedral frameworks which are themselves not disordered.

We propose four conditions applicable to the octahedral portion of the 3 Å wallpaper structures which provide adjustments to mismatches and which themselves arise from the severe restrictions placed on the spatial distribution of edge lengths by the fiber repeat. *First*, partial site occupancies such as Mg(1) and Mg(2) in pinakiolite afford a uniform expansion of the MgO<sub>6</sub> octahedra. In effect, the 2 × 3 Å repeat distance would dictate the extent of partial occupancy such as to assure the proper match with the rest of the structure. *Second*, unshared edges parallel to the fiber repeat expand on account of contracted edges which result from edge-sharing

normal to the fiber repeat. *Third*, a variety of solid solutions involving  $\text{Me}^{2+}$ ,  $\text{Me}^{3+}$ , and  $\text{Me}^{4+}$  cations can provide spatially uniform polyhedral averages. Presumably, the site distributions are dictated in the same fashion as the partial occupancies of the first condition, limited by the electrostatic sums. *Fourth*, the appearance of octahedral bundles, as in wightmanite and gageite, result in long shared edges parallel to the fiber repeat, a consequence of the long Me-O distances to the central oxide anion in the bundle. Thus, bundles can coexist with columns in the same structure, even though the latter have no shared edges parallel to the fiber repeat and even though the octahedral cations are all of the same kind.

### Acknowledgments

During construction of the manuscript, we were informed of the warwickite structure determination by Dr. F. F. Foit of the University of Washington. Dr. Foit kindly provided a preprint. Although there exist some differences in techniques and minor differences in results, we felt it prudent not to alter our manuscript since the studies constitute independent efforts.

We thank Dr. A. J. Irving for his analytical work on crystals of pinakiolite and warwickite. Discussion of the hulsite structure with Dr. J. R. Clark aided in our classification and description of pinakiolite. Finally, Professor W. A. Dollase offered many suggestions to the improvement of the manuscript.

Support of these studies include the grant GA-10932 from the National Science Foundation and a Materials Research Grant, also from NSF, awarded to The University of Chicago.

### References

- BAUR, W. H. (1970) Bond length variation and distorted coordination polyhedra in inorganic crystals. *Trans. Am. Crystallogr. Assoc.* **6**, 129-155.
- BRADLEY, W. M. (1909) On the analysis and chemical composition of the mineral warwickite. *Am. J. Sci.* **27**, 179-184.
- BURNHAM, C. W. (1966) Computation of absorption corrections, and the significance of the end effect. *Am. Mineral.* **51**, 159-167.
- CLARK, J. R. (1965) Crystallographic data for the iron borate mineral, hulsite. *Am. Mineral.* **50**, 249-254.
- CROMER, D. T., AND J. B. MANN (1968) X-ray scattering factors computed from numerical Hartree-Fock wave functions. *Acta Crystallogr.* **A24**, 321-324.
- EVANS, H. T. JR. (1971) Heteropoly and isopoly complexes of the transition elements of groups 5 and 6. *Perspectives in Structural Chemistry*, VOL. 4. Dunitz/Ibers, Eds., John Wiley and Sons, New York, p. 1-59.
- FLINK, G. (1890) XVII. Ueber Pinakiolith and Trimerit, zwei neue Mineralien aus den Mangangruben Schwedens. *Z. Krystallogr.* **18**, 361-365.
- LARSEN, E. S., AND H. BERMAN (1934) The microscopic determination of the nonopaque minerals. *U.S. Geol. Surv. Bull.* **848**, 31.
- MOORE, P. B. (1967) Crystal chemistry of the basic manganese arsenate minerals. 1. The crystal structures of flinkite,  $\text{Mn}^{2+}_2\text{Mn}^{3+}(\text{OH})_4(\text{AsO}_4)$  and retzian,  $\text{Mn}^{2+}_2\text{Y}^{3+}(\text{OH})_4(\text{AsO}_4)$ . *Am. Mineral.* **52**, 1603-1613.
- (1968) The crystal structure of chlorophoenicite. *Am. Mineral.* **53**, 1110-1119.
- (1969) A novel octahedral framework structure: gageite. *Am. Mineral.* **54**, 1005-1017.
- , AND T. ARAKI (1972) Wightmanite,  $\text{Mg}_6(\text{O})(\text{OH})_6[\text{BO}_3] \cdot n\text{H}_2\text{O}$ , a natural drainpipe. *Nature Phys. Sci.* **239**, 25-26.
- MURDOCH, J. (1962) Wightmanite, a new borate mineral from Crestmore, California. *Am. Mineral.* **47**, 718-722.
- ONKEN, H., AND K. F. FISCHER (1968) Representation and tabulation of spherical atomic scattering factors in polynomial approximation. *Z. Kristallogr.* **127**, 188-199.
- RAMACHANDRAN, G. N., AND R. SRINIVASAN (1970) *Fourier Methods in Crystallography*. Wiley-Interscience, New York, p. 96-119.
- RANDMETS, R. (1960) Orthopinakiolite, a new modification of  $\text{Mg}_3\text{Mn}^{2+}\text{Mn}^{3+}_2\text{B}_2\text{O}_{10}$  from Långban, Sweden. *Ark. Mineral. Geol.* **2**, 551-555.
- SHANNON, R. D., AND C. T. PREWITT (1969) Effective ionic radii in oxides and fluorides. *Acta Crystallogr.* **B25**, 925-146.
- TAKÉUCHI, Y., T. WATANABE, AND T. ITO (1950) The crystal structure of warwickite, ludwigite, and pinakiolite. *Acta Crystallogr.* **3**, 98-107.
- TILLMANN, E., AND W. H. BAUR (1970) A new type of polycation in heptasodiumfluoridebisarsenate-19-hydrate. *Naturwissenschaften*, **5**, 242-243.
- VENKATKRISHNAN, V., AND M. J. BUERGER (1972) The crystal structure of  $\text{FeCoOBO}_3$ . *Z. Kristallogr.* **135**, 321-338.

Manuscript received, November 15, 1973; accepted for publication, April 18, 1974.